Application of Non-Extensive Statistics in High Energy Physics

M.Sc. Thesis

By

Prateek Kumar

DISCIPLINE OF PHYSICS

INDIAN INSTITUTE OF TECHNOLOGY INDORE

May, 2016

Application of Non-Extensive Statistics in High Energy Physics

A THESIS

Submitted in partial fulfillment of the

requirements for the award of the degree

of

Master of Science

by

Prateek Kumar

DISCIPLINE OF PHYSICS

INDIAN INSTITUTE OF TECHNOLOGY

INDORE

Acknowledgements

There are lots of people I would like to thank for a huge variety of reasons. Though it is an almost impossible task but I am going to try out anyway, and if your name is not listed, rest assured that my gratitude is not less than for those listed below. It is with the deepest gratitude that I acknowledge the persistent support and guidance of my supervisor Dr. Raghunath Sahoo, Discipline of Physics, Indian Institute of Technology, Indore for giving his valuable time, guidance, co-operation and constant encouragement and providing all the necessary facilities throughout the course of my studies. His enthusiasm in research and patience in teaching touched my soul and encouraged me to march forward all these past years. I would like to express appreciation towards my lab mates espicially, Dhananjay Thakur and Sushanta Tripathy, Arvind Khuntia for the kind help they provided me. Also, I am indebted to Dr.Prakhar Garg, Dr. S.K. Tiwari & Dr. Trambak Bhattacharya, who worked as a postdoctral fellows in our group. Dr. Prakhar Garg and his extraordinary patience, problem-solving and multi-task ability has set an outstanding example. His involvement as a contact in our analysis group has also granted me the advantange to discuss with him various issues related to my research. The guidance he provided me with programming techniques, software utilization and documentation editing, will benefit me for life time. Finally, I am grateful to some more people who work as family and friends. I especially thank to Aditya Bhaiya, Pooja Didi, Pragati Didi for their support for being there always for any kind of help.

(Prateek Kumar)

Contents

List of Figures

Chapter 1

Introduction

Science is the study of the physical world and it manifestations, by using systematic observation and experimentation. Nature, on the other hand, is the actual physical world including all natural phenomena and living beings. Both are made up of rules that can be rooted in the concept that governing dynamics. The numerous forms of science investigate the nature and behavior of matter and energy on a vast range of size and scale. So the excessive enthusiasm of science maniac people is always tends to understand nature with science. Experimental High Energy Physics is one of the yardsticks of science to understand the nature & its origin.

Particularly "high-energy nuclear physics" studies the behaviour of nuclear matter in energy regimes typical of relativistic in nature. At sufficient collision energies, these types of collisions are theorized to produce the quark-gluon plasma. A high-energy collision is characterized by colliding particles, which have their momenta much higher than their rest mass and thus named as relativistic particles. A typical event of two colliding hadrons, e.g. protons, can originate tens or hundreds of particles, from a variety of processes.

Nuclear collisions have been playing an important role in high-energy nuclear physics as they provide quite unique opportunity to experimental approach of forming quark matter under extreme conditions. The Large Hadron Collider (LHC) at CERN is currently the most powerful particle accelerator. Since the start of data taking in 2009, the LHC has achieved collision energies ranging from 900 GeV up to 13 TeV for protons (p-p) and 5.02 TeV for lead ions (Pb-Pb). These energies outreach those of earlier built machines as for example, the Tevatron at FermiLab (USA) or the Relativistic Hevy-Ion Collider (RHIC) at Brookhaven National Laboratory (BNL) (USA) by a factor 4 to 14.

The spurring scientific motivations of the four main LHC experiments, ATLAS, CMS, ALICE and LHCb are very different. Though these experiments all look forward to test and enlarge the understanding of the Standard Model of particle physics, a wide spectrum of physics topics are covered by the individual collaborations. This spectrum contains the following research questions:

- Where does the mass of particles originate from ?
- What is the origin of the invisible matter in our universe, called dark matter ?
- Is super-symmetry an explanation? What does dark energy consist of ? Why is matter preferred to anti-matter in the present universe, although it should have been produced in equal amounts from the available energy after the big-bang ?
- What were the properties of matter a few microseconds after the big-bang when neither nucleons nor atoms had yet been formed ?

While ATLAS and CMS address the first two research problems by the investigation of the famous Higgs boson [1] and the search for super-symmetry particle candidates. LHCb is dedicated to the study of a potential matter-antimatter asymmetry via the determination of the mixing relation of particles and anti-particles [2]. These phenomena are expected to be best visible in p+p collisions, because in this case, the background is much smaller as compared to Pb+Pb collisions and the feasible collision energies are larger by a factor of three. Furthermore, for p+p, a sufficiently high luminosity for high enough statistics in the data can be provided. To summarise, the

[1] The Higgs boson or more precisely its Higgs field is supposed to give mass to the particles, which makes them distinguishable. It was recently discovered by ATLAS and CMS at the LHC.

main task of these three experiments is to measure the reaction products of p+p collisions.

The ALICE (A Large Ion Collider Experiment) apparatus, however, was principally designed for the investigation of relativistic Pb+Pb collisions. Here, the particle multiplicity is around 100 times larger than in p+p collisions. By the means of heavy-ion collisions, ALICE addresses questions about the state of dissolved nuclear matter during the first microseconds of the big-bang and the characteristics of matter under extreme conditions. In the following section, the motivations for the analysis of heavy-ion collisions are reviewed.

1.1 A brief history of heavy-ion collision research

The first hevy-ion collisions at modestly relativistic conditions were undertaken at the Lawrence Berkeley National Laboratory, LBNL, at Berkeley, USA, and at the Joint Institute for Nuclear Research, JINR, in Dubna, USSR. At the LBL, a transport line was built to carry hevy-ions from the hevy-ion accelerator HILAC to the Bevatron. The energy scale at the level of 1-2 GeV per nucleon attained initially, yields compressed nuclear matter at few times normal nuclear density. The demonstration of the possibility of studying the properties of compressed and excited nuclear matter motivated research programs at much higher energies in accelerators available at BNL and CERN with relativistic beams targeting laboratory fixed targets. The first collider experiments started in 1999 at RHIC and LHC begun colliding hevy-ions at one order of magnitude higher energy in 2010.

Previous high-energy nuclear accelerator experiments have studied heavy-ion collisions using projectile energies of 1 GeV/nucleon up to 158 GeV/nucleon. Experiments of this type and called "fixed target" experiments and primarily they accelerate a "bunch" of ions (typically around 10^6 to 10^8 ions per bunch) to speeds approaching the speed of light (0.999c) and smash them into a target of similar hevy-ions. While all collision systems are interesting, great focus was applied in the late 1990s to symmetric collision systems of gold beams on gold targets at Brookhaven National Laboratory's Alternating Gradient Synchrotron (AGS) and Uranium beams on Uranium targets at CERN's Super Proton Synchrotron [3].

At BNL the four primary experiments at RHIC (PHENIX, STAR, PHOBOS, and BRAHMS) study collisions of highly relativistic nuclei. Unlike fixed target experiments, collider experiments steer two [4] accelerated beams of ions toward each other at (in the case of RHIC) six interaction regions. At RHIC, ions can be accelerated (depending on the ion size) from 100 GeV/nucleon to 250GeV/nucleon. Since each colliding ion possesses this energy moving in opposite directions, the maximum energy of the collisions can achieve a centre of mass collision energy of 200GeV/nucleon for Au+Au and 500GeV/nucleon for $p+p$.

The ALICE (A Large Ion Collider Experiment) detector at the LHC at CERN is specialized in studying Pb+Pb collisions at a centre-of-mass energy of 2.76 TeV per nucleon. Other LHC detectors like CMS, ATLAS, and LHCb also have hevy-ion programs. LHC is capable of accelerating protons as well as lead ions to velocities extremly close to the speed of light. The apparent difference between the two collision systems p+p and Pb+Pb is that, the lead nucleus consists of 82 protons and 126 neutrons (=208 nucleons), the $p+p$ collisions are studied in order to acquire knowledge about specific particle production mechanism from elementary reactions. Heavy-ion collisions are the tool for investigating the nature of nuclear matter at high temperatures as well as high-energy densities. At very high energies or densities, a transformation of nuclear matter to a dissociated state of its elementary constituents is expected. This state of free quarks and gluons is called quark gluon plasma (QGP). The LHC collider at CERN operates one month a year in the nuclear collision mode, with Pb-nuclei colliding at 2.76 TeV per nucleon pair, about 1500 times the energy equivalent of the rest mass. Overall 1250 valance quarks collide generating a hot quark-gluon soup. Heavy atomic nuclei stripped of their electron cloud are called heavy-ions, and one speaks of (ultra)relativistic heavy-ions when the kinetic energy exceeds significantly the rest mass energy, as it is the case at LHC. The outcome of such collisions is the production of very strongly interacting particles.

In August 2012 ALICE scientists announced that their experiments produced quark-gluon plasma with an initial temperature at around 5.5 trillion degree Kelvin, the highest temperature achieved in any physical experiments so far[1]. This temperature is about 38% higher than the previous record of about 4 trillion degrees, achieved in the 2010 experiments at the Brookhaven National Laboratory(BNL). The quark-gluon plasma produced by these experiments approximates the conditions in the universe that existed microseconds after the Big Bang, before the matter coalesced into atoms [5].

If we think about QGP, it is not a stationary medium but subjected to dynamical evolution. The expansion of the system leads to a cooling followed by the final formation of hadrons, which are particles built from the available quarks and gluons. These newly created particles, consisting either of three quarks (baryons) or of a quark and an anti-quark pair (mesons) are eventually measured by a detector. In addition to the hadrons, leptons (i.e. electrons, photons) are produced. Since the whole collision evolution with a duration of 10^{-23} sec is technically not possible to be followed, observables are vital that reveal the characteristics of the medium and the underlying processes during the different evolution phases.

In order to shed light on the characteristics of matter in a QGP state, a lot of energy is needed to crack the nuclei and their nucleons into their elementary particles, the quarks and gluons. Until now, the critical temperature of the phase transition to the QGP has not yet been determined exactly. Nonetheless temperature estimates yield values of 100 - 200 MeV, roughly corresponding to 10^{12} K, which is a hundred thousand times hotter than the core of the sun. Moreover, the spatial scale of a heavy-ion collision is about a few femtometer leading to extremely high-energy densities

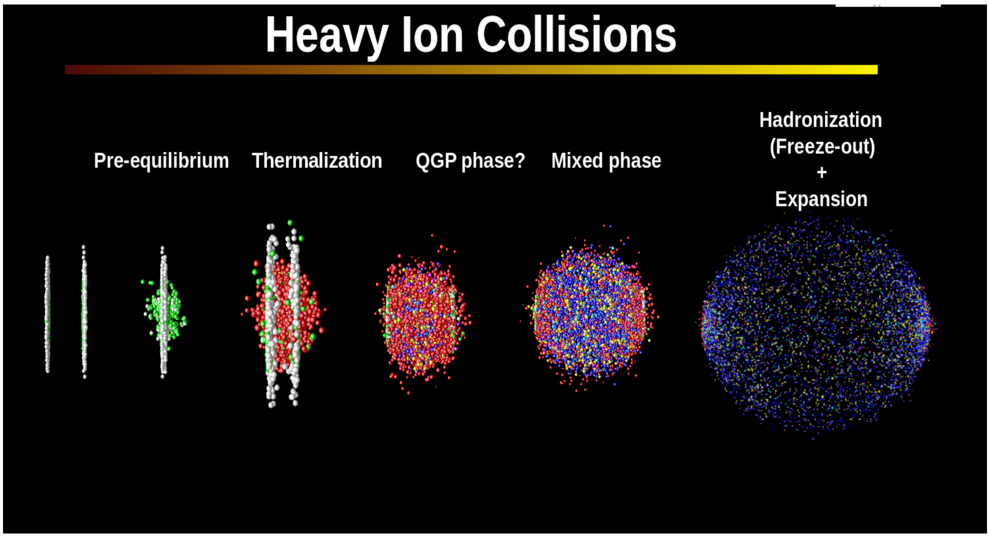

Figure 1.1. Schematic of space-timeevolution of Heavy-ion Collision

(pressures) as compared to ground state nuclear matter. The nature of quark matter at extreme high-energy density, which is believed to exist in the early universe in a few s after the Big-Bang, is one of the most interesting themes not only for cosmologists but also for particle and nuclear physicists because a new form of quark matter is theoretically expected to be created at a high-energy density.

1.2 QGP in the laboratory: Ultra-relativistic hevy-ion collisions

The experimental link between the QCD phase transition and the measurement of temperature, pressure and energy density of the deconfined phase, is ultra-relativistic heavy-ion collisions. At high-energy, thousands of partons(quarks and gluons) produced in these collisions create a fireball in local thermal equilibrium that rapidly expands and cools down. For high-energy in the centre-of-mass of the collisions, the fireball is initially made up of interacting quarks and gluons that hadronize only when the system temperature falls below the temperature needed for the phase transition to occur (critical temperature). As the two heavy-ions collide at very high energies, they deposit a substantial part of their kinetic energy into a small region of space. Depending on the energy density achieved, the initial state of the system will be either in the form of a QGP or a hot/dense hadronic gas. The evolution of an heavy-ion collision with an intermediate state of a nucleus-nucleus collision at relativistic energy passes through different stages. Schematic picture of different staged of the collisions are shown in Fig. (1.1). One can broadly classify the space-time evolution into the following stages:

a.)Pre-equilibrium stage: Initial partonic collisions produce a fireball in a highly excited state. In all possibility, the fireball is not in equilibrium. Constituents of the system collide frequently to establish a local-equilibrium state. The time takes to establish local equilibrium is called thermalisation time.

b.) Thermalization & **QGP:** In the equilibrium or the thermalised state, the system has thermal pressure, which acts against the surrounding vacuum. The system then undergoes collective (hydrodynamic) expansion. As the system expands, its density (energy density) decreases and the system cool down. Assuming that the interactions of quarks and gluons are sufficiently small at the temperatures achieved in heavy-ion collisions, the energy density, pressure etc. can be calculated in QCD using thermal perturbation theory. Driven by the high internal pressure, the thermalized QGP expands according to the laws of relativistic hydrodynamics [7]. The most important question that arises during this part of the evolution is that of chemical equilibration of the partons. It is generally believed that gluons, because of their larger colour degeneracy equilibrate chemically much faster than the quarks. It is found that even light quark flavours fail to achieve chemical equilibrium during the lifetime of the plasma [8, 9].

c.) Hadronization and the mixed phase: Expansion of the QGP proceeds till the critical temperature T_c is reached. At this instant, the phase transition to hadronic matter starts. Through the process of hadronization the coloured particles - quarks and gluons combine to form colour-neutral hadrons. The order of the transition is still a matter of debate . In case of a possible first order phase transition the released latent heat maintains the temperature of the system at T_c even though the system continues to expand. This mixed phase persists until all the matter has converted to the hadronic phase.

d.) The hadronic phase and freeze-out: Hadronic matter also stay in thermal equilibrium. Constituent hadrons collide with each other to maintain local equilibrium. The system expand and cools down. A stage comes when inelastic collisions, in which hadrons changes identity, become too small to keep up with expansion. The stage is called chemical freeze-out. Hadron abundances remain fixed after the chemical freeze-out. However, due to elastic collisions, local equilibrium can still be maintained and system cools and expands with fixed hadron abundances. Eventually a stage comes when average distance between the constituents will be larger than the syatem size. Collisions between the constituents will be so rare that local thermal equilibrium can not be maintained. The hydrodynamic description hence break down. The hadrons decouple or freeze-out. It is called kinetic freeze-out. Hadrons from the freeze-out surface will thus be detected in the detector.

1.2.1 QCD Phase Diagram

The phase diagram of quark matter is not well known, either experimentally or theoretically. A commonly conjectured form of the phase diagram is shown in the Figure 1.2. It is applicable to matter in a compact star, where the only relevant thermodynamic potentials are quark chemical potential, μ_B and temperature, T. For guidance it also shows the typical values of μ_B and T in heavy-ion collisions and in the early Universe. Higher μ_B means a stronger bias favoring quarks over antiquarks. At low temperatures there are no antiquarks, and then higher μ_B generally means a higher density of quarks.

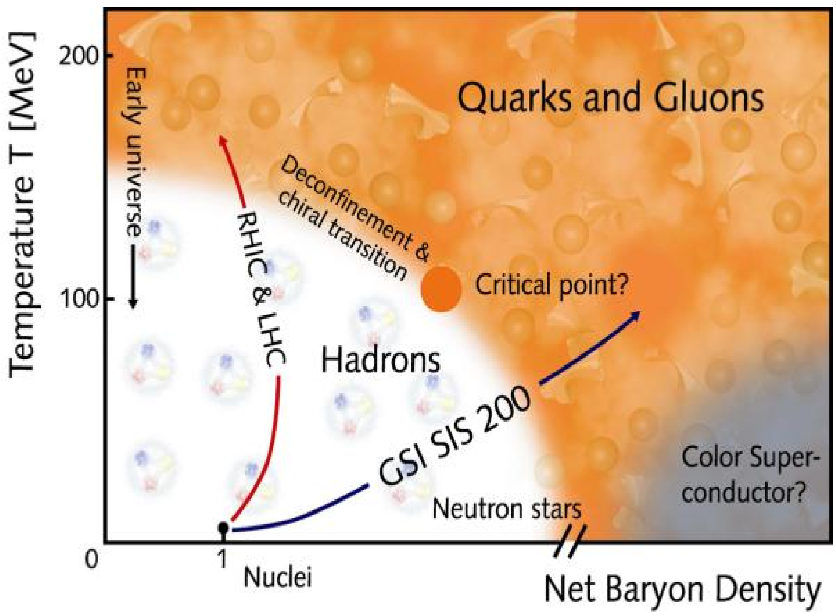

Figure 1.2. A schematic of the QCD phase diagram of nuclear matter in terms of the temperature (T) and baryon chemical potential (μ_B). The possible location of the critical point is indicated as the point at which the sharp distinction between the hadronic gas and QGP phases ceases to exist.

Along the **horizontal axis** the temperature is zero, and the density rises from the onset of nuclear matter through the transition to quark matter. Compact stars are in this region of the phase diagram, although it is not known whether their cores are dense enough to reach the quark matter phase.

Along the **vertical axis** the temperature rises, taking us through the crossover from the hadronic gas, in which quarks are confined into neutrons and protons, to the quark gluon plasma (QGP), in which quarks and gluons are deconfined. This is the region explored by high-energy heavy-ion colliders such as the Relativistic Heavy-Ion Collider (RHIC) and Large Hadron Collider (LHC).

On the basis of thermodynamical considerations and QCD calculations, strongly interacting matter is expected to exist in different states. Its behaviour can change for different conditions of temperature and baryonic chemical potential (μ_B). The baryo-chemical potential is defined as the energy (E) needed to increase of one unit the total number of baryons and anti-baryons. Figure 1.2 shows an illustration of the phase diagram of nuclear matter, varying its temperature and baryo-chemical potential.

At low temperatures and for $\mu_B \approx m_p \approx 940$ MeV, nuclear matter is in its standard conditions (atomic nuclei). Increasing the energy density of the system, "heating" the nuclear matter (upward in the plot) or increasing the baryo-chemical potential (going towards right in the diagram), a state of QGP phase is reached. Going the other way, one obtain hadronic phase in this state, nucleons interact and form pions, excited states of the protons and neutrons (Δ resonances) and other hadrons. If the energy density is further increased, a deconfined Quark Gluon Plasma (QGP) phase is predicted. The density of gluons and quarks, in this phase, becomes so high that partons are still interacting but not confined within hadrons anymore. For extreme values of baryo-chemical density, nuclear matter should be in conditions of quark colour superconductivity.

There are many paths on the phase diagram, that the phase transition can follow, varying the temperature and the baryo-chemical potential. In the early Universe, for example, the transition from a QGP phase to hadron matter took place for $\mu_B \approx 0$ as a consequence of the Universe expansion and the decrease of its temperature. In that case, the transition phase evolved from a deconfined state of partons to hadronic matter. On the other hand, in the formation of neutron stars, the gravitational collapse causes an increase in the baryonic density for temperature very close to zero.

The phase transition is characterized by how fast the free energy of the system is varied, for a neighborhood of the transition temperature. The transition between different states belongs to the first order, if it happens with a discontinuos pattern in the first derivatives of the free energy. If the phase transition occurs with discontinuos higher derivatives after the first, it is a second order transition. Second order transitions are, for example, the ferromagnetic transition or the superfluid transition. Phase transitions can also occur without fast modification of the parameters of the system, so with a continuos behaviour for the free energy and its derivatives. These transitions are called “cross-over”. In peculiar conditions of thermodynamic parameters, the process can pass from a first to a second order transition. These conditions are called critical points and usually two states of matters coexist.

1.3 The QGP Signatures

There are many observable to understand the formation of QGP. Here we outline some of the QGP signatures. The signatures of the QGP can be divided in different categories, related to the different stages considered by the evolution picture described before- the deconfined medium (QGP), a possible interacting hadronic medium, and the final hadronic state [14].

1.3.1 Heavy-quark and quarkonium production

Among the hard probes that could provide direct information on the deconfined medium produced in the heavy-ion events, charm and bottom quarks are very suitable to understand the dynamics of the collisions. Their production takes place on a timescale of the order of $1/m_Q$, where m_Q is the heavy-quark mass. On the other hand, thanks to their long lifetime, charm and bottom quarks can live through the thermalization phase and carry information about the system. In order to extract information about the plasma from the features of heavy-quarks production in heavy-ion collisions it is very important to well understand their production in $p+p$ and A-A interactions and compare some observables like the total production rates, the transverse momentum distributions and the kinematic correlations between the heavy quarks and antiquarks. Both the productions of bound states of $c\bar{c}$ and $b\bar{b}$ (quarkonia) and of open charm and bottom will be extensively studied by ALICE & RHIC, either as different probes of the event evolution. The study of the correlations between the properties of open charm and bottom and quarkonia spectra will allow to understand the dynamics of the dense medium. In the very low p_T region, which will be accessible to ALICE, the production of heavy quark-antiquark pairs should increase the probability of forming quarkonia. In the region of perturbative production, i.e. at large p_T , the quarkonium suppression should take place. Moreover, the different effects of enhancement in the productions of quark-antiquark pairs and of the quarkonium suppression, should be disentangled by the study of the correlations between quarkonium and open heavy-quarks momentum spectra.

1.3.2 Open charm and beauty observation

The measurement of open charm and open beauty production allows one to investigate the mechanisms of heavy-quarks production, propagation and, at low momenta, hadronization in the hot and dense medium formed in high-energy nucleus-nucleus collisions. The open charm and open beauty cross sections are also needed as a reference to measure the effect of the transition to a deconfined phase on the production of quarkonia. A direct measurement of the D and B mesons yields would provide the normalization for charmonia and bottomonia production. Finally, the measurement of B meson production is necessary within the search for the quarkonia suppression, in order to estimate the contribution of secondary J/ψ (from $B \to J/\psi + X$) to the total J/ψ yield: B mesons decay into J/ψ mesons. Direct J/ψ production might be further suppressed by QGP because of Debey's screening, secondary J/ψ mesons are conceivably contributing a large fraction to the observable J/ψ signal. The measurement of charm and beauty production in proton-proton and proton-nucleus collisions, besides providing the necessary baseline for the study of medium effects in nucleus-nucleus collisions, is intrinsically interesting as a test of both perturbative and non-perturbative sectors of QCD in a new energy domain.

1.3.3 High-$\mathrm{p_T}$ Suppression and Jet Quenching

In 1982 Bjorken stated that an high-$\mathrm{p_T}$ quarks or gluons might lose their initial transverse momentum while plowing through quark-gluon plasma [14].

Hard partons traversing the hot and dense medium created in heavy-ion collisions lose energy by gluon radiation and/or colliding elastically with surrounding partons [25, 26]. This would have many observable consequences, of which the most directly measurable would be a depletion in the yield of high-p_T hadrons [27, 28]. One of the most exciting results to date at RHIC is that the yield of π^0 at high transverse momentum in central $\sqrt{s_{NN}}$=200 GeV Au+Au collisions is suppressed compared to the yield in $p+p$ collisions scaled by the number of underlying nucleon-nucleon collisions [20]. This shown in Figure 1.3. The phenomenon is interpreted as a consequence of the so called jet quenching effect. Nuclear effects on hadron production in d-Au and Au-Au collisions are measured through comparison with the yeild in p+p collisions Equation (1.1). In hadronic collisions, hard parton scatterings occurring in the initial interaction produce cascades of consecutive emissions of partons, called $jets$. The jets fragment in hadrons during the hadronization phase. The jets lose their energy while propagating in the hot and dense medium due to the gluon radiations, resulting in the suppression of hard jets (the so-called $jet-quenching$ effect). Nuclear Modification Factor, R_{AA} is defined as:

$$R_{AA} = \frac{1/N_{evt}^{AA} d^2 N_{ch}^{AA}/d\eta dp_T}{\langle N_{coll} \rangle \, 1/N_{evt}^{pp} d^2 N_{ch}^{pp}/d\eta dp_T} \tag{1.1}$$

where η is the pseudorapidity, N_{evt}^{AA} and N_{evt}^{pp} are the number of A+A and p+p events and $\langle N_{coll} \rangle$ is the mean number of binary nucleon-nucleon collisions. High-energy nucleus-nucleus collisions allow to study the properties of this medium through modifications of the jet-structure:

- **Suppressed particle yield:** The in-medium energy loss results in a suppression of the hard jets and in a reduction of the high-p_T particles yields.

- **Impact parameter dependence:** Since the characteristics and the size of the dense medium should depend on the centrality of the initial collision, a correlation of the jet quenching effect with the impact parameter is expected to be observed.

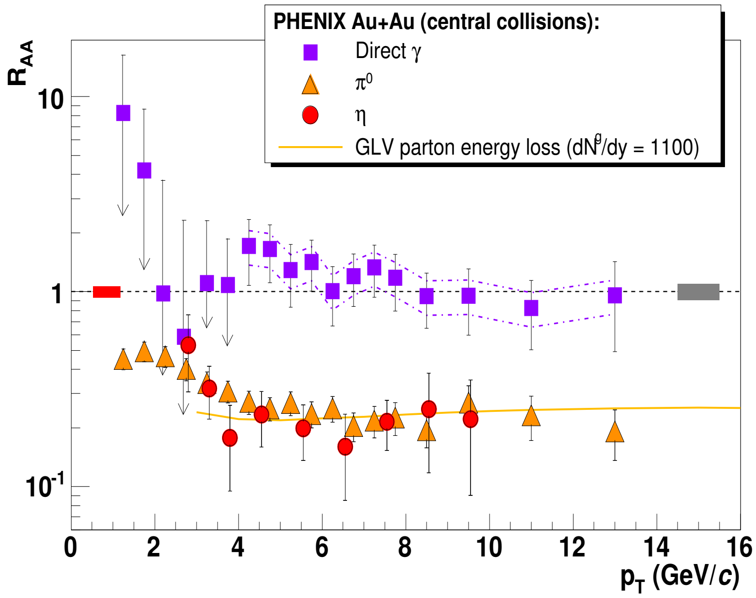

Figure 1.3. Nuclear modification factor R_{AA} of mesons π^0 (triangles), η (circles) and direct photons (squares), as measured by PHENIX [20]

The RHIC experiments were the first to observe the suppressed production of high-p_T hadrons in central A+A collisions, i.e. Au+Au at $\sqrt{s_{\rm NN}}$=200 GeV [15, 16]. High-$\rm p_T$ hadrons are generally produced in the fragmentation of high-$\rm p_T$ partons created in the early stages of a collision but in the presence of the QGP these partons loose energy as they propagate through. In effect, the hot and dense medium modifies the hadron $\rm p_T$ spectra, reducing the yield at high momenta. This is measured by comparing the yield in A+A collisions to the yield in nucleon-nucleon (e.g. $p+p(\bar{p})$ at the same centre-of-mass energy per nucleon. Figure (1.4) shows the STAR, PHENIX and the recent ALICE measurement of the so called nuclear modification factor R_{AA} , defined define in Eq. (1.1) In the 5% most central Pb+Pb collisions at $\sqrt{s_{\rm NN}}$= 2.76 TeV the R_{AA} is significantly less than 1, reaching a minimum at $\rm p_T \approx 6$ GeV/c. In the case of no suppression (or enhancement) of the high- $\rm p_T$ hadron production the R_{AA} would be equal to 1.

The measurement of the R_{AA} factor has motivated a detailed analysis of the jet structure at RHIC which has led to the discovery of another effect related to high-$\rm p_T$ suppression in the plasma: jet quenching [14, 15].

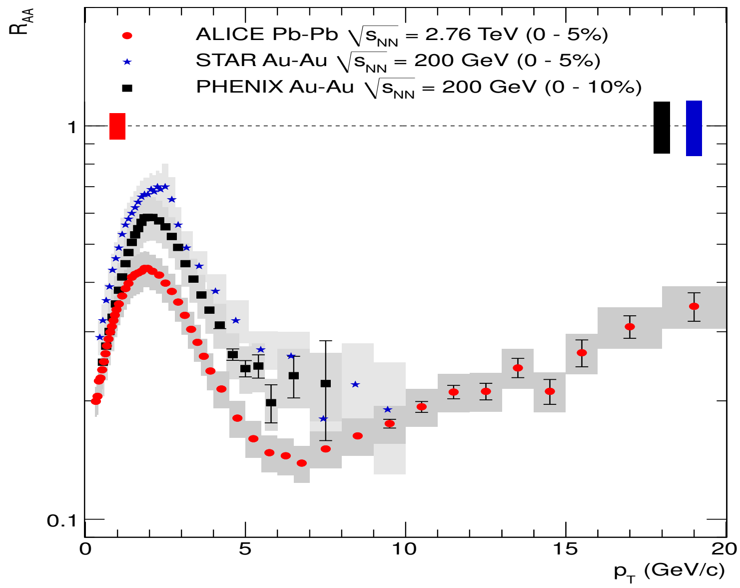

Figure 1.4. Nuclear modification factor, R_{AA} , in central Pb+Pb collisions at $\sqrt{s_{\rm NN}}$=2.76 TeV (ALICE) and Au-Au collisions at $\sqrt{s_{\rm NN}}$=200 GeV by the PHENIX and STAR experiments at RHIC. The figure is taken from [17]

1.3.4 Charmonium Suppression

It was predicted by Matsui and Satz [18] that the yield of charmonium states ($c\bar{c}$) will be suppressed if the QGP is formed. Due to the effects of Debye screening in the QGP, bound states with a large radius relative to the Debye radius, r_D , such as the J/ψ meson, will be dissociated. Because the mass of the charm quark is much greater than that of the up, down and strange quarks, $c\bar{c}$ states are almost exclusively produced during the early stages of the collision. If the QGP is formed, and at high enough temperature, $c\bar{c}$ bound state will exhibit an apparent suppression in the final state hadron spectra while at the same time the disassociated charm quarks enhance the open charm production (e.g. $D^{\pm}$, D^0). J/ψ suppression was first confirmed at the SPS [19], and more recently at RHIC [20]. Interestingly, while at the SPS and RHIC the suppression is at a similar level, at LHC it is measured to be less [21]. There are several models which try to explain this apparent enhancement in the J/ψ yield by considering recombination of deconfined charm quarks during the hadronisation process [22, 23].

At high energy $\rm p_T$-specturm follow a Tsallis type of non-extensive statistical distribution; in the following chapter, we have made an attempt to study the R_{AA} in the framework of non-extensive statistics using Boltzmann Transport Equation with Relaxation time approximation.

Chapter 2

Tsallis Statistics

In the present work, our quest is to study the matter formed in hadronic and heavy-ion collision, which may be described in terms of equilibrium or non-equilibrium statistical mechanics. At high energies, when the particle produce this is dominated by purturbative Quantum Chromo Dynamics (pQCD), the $\mathrm{p_T}$-spectra is better described by ba non-extensive Tsallis statistics. The well-known Boltzmann equilibrium statistics is an approximation of this Tsallis super-statistics [40]. The later is used to study syatems, which are away from eqilibrium with a non-extensive parameter q to quantify the degree of non-equilibrium. In 1988, Tsallis postulated a generalization of the Boltzmann-Gibbs-Shannon entropy, now popurarly called the Tsallis Entropy. Tsallis entropy is non-extensive, which means that if two identical systems combine, the entropy of combined system is not equal to summation of entropy of its subsystems.

2.1 Boltzmann-Gibbs Statistics

In statistical mechanics, Boltzmann's equation is a probability equation relating the entropy S of an ideal gas to the quantity W, which is the number of microstates corresponding to a given macrostate:

$$S = k_B \ln W, \tag{2.1}$$

where k_B is the Boltzmann constant. In short, the Boltzmann formula shows the relationship between entropy and the number of ways the atoms or molecules of a thermodynamic system can be arranged. For an ideal gas of N identical particles, of which N_i are in the i^{th} microscopic condition (range) of position and momentum. For this case, the probability of each microstate of the system is equal, W can be counted using the formula for permutations:

$$W = N! \;/\; \prod_i N_i! \tag{2.2}$$

where i ranges over all possible molecular conditions.

For thermodynamic systems where microstates of the system may not have equal probabilities, the appropriate generalization, called the Gibbs entropy, is:

$$S = -k_{\mathrm{B}} \sum p_i \ln p_i$$

This reduces to equation (2.1) if the probabilities are all equal.

2.2 Tsallis Entropy:: Generlized Version of Boltzmann Gibbs Entropy

Traditionally the bulk of spectra in both $p+p$ and heavy-ion collisions are described using a boltzmann like, thermal distribution with an inverse slope parameter called "temprature". The Tsallis distribution which describes systems away from thermal equilibrium is now widely used to describe particle spectra in hadrons and heavy-ion collisions. The Tsallis distribution describes a system in terms of two parameters; "temperature" and "q" which measures deviation from thermal distribution. It has been shown that the functional form of the Tsallis distribution in terms of parameter q is the same as the QCD-inspired Hagedorn formula in terms of power n [55].

$$h(p_T) = C\left(1 + \frac{p_T}{nT}\right)^{-n} \longrightarrow \begin{cases} \exp\left(-\frac{p_T}{T}\right) & \text{for } p_T \to 0, \\ p_T^{-n} & \text{for } p_T \to \infty, \end{cases} \tag{2.3}$$

Both n and q are related and describe the power law tail of the hadron spectra coming from QCD hard scatterings. This was first proposed in [10] as the simplest formula extrapolating the large power behavior expected from parton collisions to exponential behavior observed for low p_T.

In a more general way, we can describe it as Boltzmann-Gibbs (BG) statistics is based on the fact that the particles with in a system interact over extremely small length scales, *i.e.* the interactions are purely collisional. Such characteristic short range interactions allow us to view the fluid as non-interacting and in turn, we generate the familiar results of statistical mechanics. It is currently well established that there are numerous physical systems under which BG statistics encounters many difficulties. Some of these physical systems which include situations characterized by long-range interactions, long-range microscopic memories, and those involving a space-time (and phase space) exhibiting a (multi)fractal structure are discussed in Ref [37]. In particular, while analysing the transverse momentum (p_T) spectra of hadrons it is found that the spectra decrease far slower than predicted by BG statistics, and appear to follow some power-law at high-p_T. Such departures from the BG exponential are argued as being attributable to dynamical effects. Essentially, these effects survive the equilibration process and can show up as apparent departures from the assumed thermal equilibrium in the form of the enhancement of the exponential tail into power-law tail. Typically, when such observations are made, one assumes that the statistical model is too simplistic and accounts for the departure via inclusion of some additional (non-equilibrium) dynamical considerations. In an attempt to overcome at least some of the difficulties experienced due to the shortcomings of BG statisitics, a generalized form of the entropy was postulated in [38]. The form of the entropy is given by:

$$S = \frac{1 - \sum_{i=1}^{W} p_i^q}{q-1} \tag{2.4}$$

p_i stands for probability for occupation of i^{th} state of the system, W counts the known microstates of the systems and q is a positive real parameter or we can say q is a "non-extensive parameter". It can be easily shown that this newly postulated entropy is nonextensive. To show that let's consider we have two independent systems A and B described by the proposed entropy in given by (2.4)

$$S_q(A) = \frac{(1-\sum_i p_{A,i}^q)}{q-1} \qquad S_q(B) = \frac{(1-\sum_i p_{B,i}^q)}{q-1} \tag{2.5}$$

then the entropy of the combined system is given by:

$$\begin{aligned} S_q(A+B) &= \frac{(1-\sum_k p_{A,B,k}^q)}{q-1} \\ &= \frac{(1-\sum_i \sum_j p_{A,i}^q \quad p_{B,j}^q)}{q-1} \\ &= \frac{(1-\sum_i \sum_j p_{A,i}^q \quad p_{B,j}^q)}{q-1} \\ &= \frac{2-\sum_i p_{A,i}^q - \sum_j p_{B,j}^q - (1-\sum_i p_{B,j}^q)(1-\sum_j p_{B,j}^q)}{q-1} \\ &= \frac{(1-\sum_i p_{A,i}^q)}{q-1} + \frac{(1-\sum_i p_{B,i}^q)}{q-1} - (q-1)\frac{(1-\sum_i p_{A,i}^q)}{q-1}\frac{(1-\sum_i p_{B,i}^q)}{q-1} \\ &= S_q(A) + S_q(B) + (1-q)S_q(A)S_q(B) \end{aligned} \tag{2.6}$$

Evidently the third term in (2.3) makes the entropy non-extensive. Furthermore, if we allow for $q \to 1$ we have:

$$\begin{aligned} S_1 &= \lim_{q\to 1} S_q \\ &= \lim_{q\to 1} S_q \\ &= \lim_{q\to 1} k\frac{(1-\sum_{i=1}^W p_i p_i^{q-1})}{q-1} \\ &= \lim_{q\to 1} k\frac{(1-\sum_{i=1}^W p_i p_i^{q-1})}{q-1} \\ &= \lim_{q\to 1} k\frac{(1-\sum_{i=1}^W p_i \exp\left[(q-1)\ln(p_i)\right]}{q-1} \end{aligned} \tag{2.7}$$

Then we can perform a Taylor expansion [13] of the exponential term in

(2.4) about $q = 1$ to give,

$$S_1 = \lim_{q\to 1} \frac{1 - \sum_{i=1}^{W} p_i[1 + (q-1)\ln P_i + \frac{(q-1)^2(\ln P_i)^2}{2!} + \frac{(q-1)^3(\ln p_i)^3}{3!} + ...]}{q-1}, \tag{2.8}$$

and using the fact that $\sum_{i=1}^{W} p_i = 1$, Eqs. 2.8 becomes:

$$\begin{aligned} S_1 &= \lim_{q\to 1}\left[-\sum_{i=1}^{W} p_i \ln p_i - \sum_{i=1}^{W} p_i \frac{(q-1)(\ln p_i)^2}{2!} - \sum_{i=1}^{W} p_i \frac{(q-1)^2(\ln p_i)^3}{3!} + ...\right], \\ &= -\sum_{i=1}^{W} p_i \ln p_i \end{aligned} \tag{2.9}$$

Evidently from Eq. (2.9), it is apparent that as $q \to 1$ the generalised non-extensive Tsallis entropy tends towards the familiar extensive Shannon-Gibbs entropy. It is clear from this, that q is some measure of the non-extensivity of the entropy of the system. Unfortunately, it does not reveal the cause of this departure from the standard Shanon-Gibbs entropy. This must be deduced from the physicsl system under consideration. Using the entropy expressed in Eqs. (2.9), we can reformulate the different distributions, at equilibrium, characterised by the different ensembles within the framework of Tsallis statistics. In a similar vain to that of BG statistics we maximise the Tsallis entropy subject to the constraints associated with the particular ensemble of interest.

2.3 Difference between Tsallis and Boltzmann and Connection between them

We already know that Tsallis entropy is a generalization of the standard Boltzmann-Gibbs entropy. The Tsallis entropy reduces to the Boltzmann and Gibbs entropies when the system is extensive, but is different otherwise. The motivation behind this is to show that the Tsallis entropy works well in situations where the Boltzmann and Gibbs entropies allegedly break down. The system governed by long-range force systems like self-gravitating systems are supposed to be one examples. Non-extensive statistical mechanics which is established by optimization of Tsallis entropy in presence of appropriate constraints, can interpret properties of many physical systems.

2.3.1 The Boltzmann-Gibbs Model

For particles radiated from a small equilibrated thermal source with temperature T we can apply Boltzmann-Gibbs statistics to describe an invariant momentum spectrum. This gives the familiar expression in Equation (2.10) where the chemical potential and spin-isospin-degeneracy factor has been dropped because we are not interested in the overall scaling factor,

$$E\frac{d^3N}{dp^3} = \frac{d^3N}{p_T dy dp_T d\phi} = \frac{d^3N}{2\pi m_T dm_T dy} \tag{2.10}$$

$$\Rightarrow \frac{d^2N}{dm_T dy} \propto m_T e^{-m_T/T},$$

where m_T is the transverse mass given by $\sqrt{p_T^2 + m^2}$. This model exhibits a turnover at low-p_T followed by qualitatively exponential fall-off(as seen in Fig. (2.1)). This captures the basic behavior of the particle spectra and gives a reasonable approximation of the p_T distribution.

2.3.2 The Blast-Wave Model

In the low p_T region experimentally measured transverse momentum spectra are well described by the blast-wave model, which applies longitudinal and transverse flow to thermal emission [43]. The model is derived by integrating the superposition of Lorentz boosted Boltzmann-Gibbs invariant momenta spectra over the freeze-out hyper surface. The model assumes boost-invariant Bjorken longitudinal expansion in a region around midrapidity and allows for an arbitrary azimuthally-symmetric velocity profile [44]. If temperature and transverse flow do not depend on the longitudinal position in a longitudinally-comoving coordinate system then the transverse momentum spectrum factorizes and can be expressed independently of longitudinal flow as

$$\frac{dN}{dp_T p_T} \propto \int_0^R r dr m_T I_0\left(\frac{p_T \sinh\rho}{T}\right) K_1\left(\frac{m_T \cosh\rho}{T}\right) \tag{2.11}$$

where ρ is the Lorentz boost angle $\tanh^{-1}\beta_r$ where β_r is the surface velocity for a given radius r and T is the freeze-out temperature. The shape of thermal spectra that depends on only the two physically meaningful parameters β and T.

2.3.3 The Tsallis Model and its connection with Boltzmann-Gibbs

At intermediate to high-$\mathrm{p_T}$ ($\mathrm{p_T} > 1-2$ GeV/c) the thermal assumption of both the simple and blast-wave models breaks down as hard processes become the dominant source of particle production. The spectra in this region is known to exhibit power-law rather than exponential behavior [45]. A generalization of the Boltzmann distribution known formally as a q-exponential captures this power-law behavior at high-$\mathrm{p_T}$ and exponential behavior at low-$\mathrm{p_T}$. This distribution, with or without the $\mathrm{m_T}$ factor, is more often called a Tsallis distribution in nuclear physics, after the Tsallis statistics from which it is derived [46].

$$\frac{d^2N}{2\pi m_T dm_T dy} \propto \left(1 + \frac{q-1}{T} m_T\right)^{-1/(q-1)} \tag{2.12}$$

Equation (2.12) gives the form of the Tsallis distribution which converges to Equation (2.10) as the non-extensivity parameter q goes to 1. This functional form has been shown to fit well both low and high p_T spectra at RHIC and LHC energies [43, 52, 53]. It could simply be a convenient functional form that evolves from exponential to power-law behavior as the physics shifts from soft to hard or it might be related to deeper physics such as anomalous diffusion or temperature inhomogeneities in the collisions [46].

In either case, it offers a model for fitting spectra that is more applicable across a broad p_T range, which we have discussed earlier.

2.4 Transverse Momentum Spectra

In high energy collisions particle spectra are studied by calculating the invariant cross-section given by (2.10)

$$E\frac{d^3N}{dp^3} = \frac{d^2N}{2\pi p_T dp_T dy},$$

where E is the energy of the particle. The mean particle yields are usually extracted from the p_T distribution of $\frac{d^2N}{dp_T dy}$ by using an appropriate parametrisation.

In first approximation, the exponential-like shape of the transverse spectra can be described using Boltzmann-Gibbs statistics [55],

$$\frac{d^2N}{2\pi p_T dp_T dy} = Ae^{-\frac{m_T}{T}} \tag{2.13}$$

where A is a normalisation parameter and $m_T = \sqrt{m^2 + p_T^2}$ is the transverse mass.

A much better description of the data is provided by the Tsallis distribution [38], often referred to as Levy-Tsallis. Based on the ideas of non-extensive thermodynamics, it is derived from the so-called Tsallis entropy S_q a generalised case of the Boltzmann-Gibbs entropy, S_{BG}:

$$S = \frac{1 - \sum_{i=1}^{W} p_i^q}{q-1} \overset{q\to 1}{S}_{BG} = -\sum_i p_i \ln p_i$$

where q is a measure of the non-extensivity of the system, hence its divergence from Boltzmann-Gibbs statistics. In the limit $q \to 1$ the entropy takes its usual form, $S_q = S_{BG}$. The successful application of the non-extensive thermodynamics in high energy physics, can be understood in terms of the finite size and the non-homogeneity of the multi-particle systems, created in elementary and heavy-ion collisions. Using equation (2.59) which we describe in section (2.6) [58], we get,

$$\begin{aligned} E\frac{d^3N}{dp^3} &= \frac{1}{2\pi p_T}\frac{d^2N}{dydp_T} \\ &= \frac{dN}{dy}\frac{(n-1)(n-2)}{2\pi nC[nC+m(n-2))]}(1+\frac{m_T-m}{nC})^{-n} \end{aligned} \tag{2.14}$$

where $n \to \frac{q}{q-1}$, $nC \to \frac{T+m_0(q-1)}{q-1}$, $m_T = \sqrt{p_T^2+m^2}$ is the transverse mass. m, $\frac{dN}{dy}$, n and C are fitting parameters. Using them we get the final expression as follows [59],

$$\begin{aligned} \frac{d^2N}{dp_T\,dy} = \quad & p_T\frac{\mathrm{d}N}{\mathrm{d}y}\frac{(n-1)(n-2)}{nC(nC+m_0(n-2))}\left[\frac{T}{T+m_0(q-1)}\right]^{-q/(q-1)} \\ & \left[1+(q-1)\frac{m_T}{T}\right]^{-q/(q-1)}. \end{aligned} \tag{2.15}$$

Using the above equation (2.15) we compare the two distribution in figure (2.1). One can clearly see that Tsallis distribution describes well the π^+ $\mathrm{p_T}$ spectra in $p+p$ collisions at $\sqrt{\mathrm{s}}$=900 GeV at LHC. On the other hand, Boltzmann distribution shows a clear deviation at high-$\mathrm{p_T}$

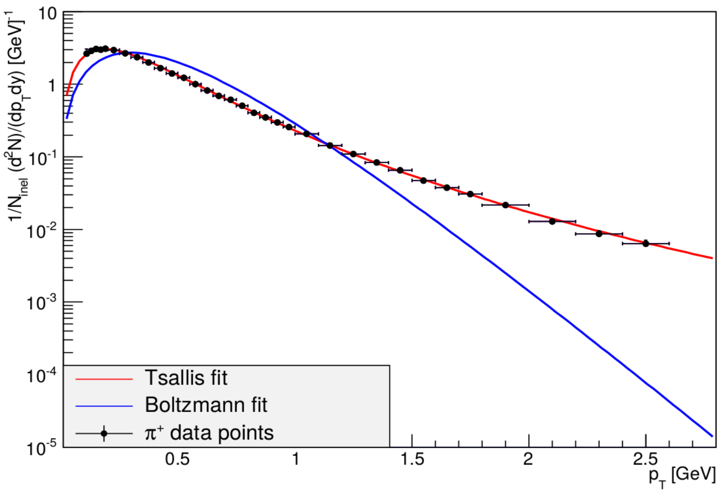

Figure 2.1. Comparison of the two distributions, Boltzmann and Tsallis. The data are $p+p$ collision at $\sqrt{\mathrm{s}}$=900 GeV taken by ALICE experiment [21]

2.5 Thermodynamics

The first law of thermodynamics postulates that the changes in the total energy of a thermodynamic system must result from: heat exchange, the mechanical work done by an external force, and from particle exchange with an external medium. Hence the conservation law relating the small changes in state variables, E, V, and N is

$$\delta E = \delta Q - P\delta V + \mu\,\delta N, \tag{2.16}$$

where P and μ are the pressure and chemical potential, respectively, and δQ is the amount of heat exchange.

The heat exchange takes into account the energy variations due to changes of internal degrees of freedom that are not described by the state variables. The heat itself is not a state variable since it can depend on the past evolution of the system and may take several values for the same thermodynamic state. However, when dealing with reversible processes (in time), it becomes possible to assign a state variable related to heat. This variable is the entropy, S , and is defined in terms of the heat exchange as $\delta Q = T\delta S$, with the temperature T being the proportionality constant. Then, when considering variations between equilibrium states that are infinitesimally close to each other, it is possible to write the first law of thermodynamics in terms of differentials of the state variables,

$$dE = TdS - PdV + \mu\,dN. \tag{2.17}$$

Hence, using Eq. (2.17), the intensive quantities, T, μ and P, can be obtained in terms of partial derivatives of the entropy as

$$\left.\frac{\partial S}{\partial E}\right|_{N,V} = \frac{1}{T}, \qquad \left.\frac{\partial S}{\partial V}\right|_{N,E} = \frac{P}{T}, \qquad \left.\frac{\partial S}{\partial N}\right|_{E,V} = -\frac{\mu}{T}. \tag{2.18}$$

The entropy is mathematically defined as an extensive and additive function of the state variables, which means that

$$S(\lambda E, \lambda V, \lambda N) = \lambda S(E, V, N). \tag{2.19}$$

Differentiating both sides with respect to λ, we obtain

$$S = E \left.\frac{\partial S}{\partial \lambda E}\right|_{\lambda N, \lambda V} + V \left.\frac{\partial S}{\partial \lambda V}\right|_{\lambda N, \lambda E} + N \left.\frac{\partial S}{\partial \lambda N}\right|_{\lambda E, \lambda V}, \tag{2.20}$$

which holds for any arbitrary value of λ. Setting $\lambda = 1$ and using Eq. (2.18), we obtain the so-called Euler's relation

$$E = -PV + TS + \mu N. \tag{2.21}$$

Using Euler's relation, Eq. (2.21), along with the first law of thermodynamics, Eq. (2.17), we arrive at the Gibbs-Duhem relation

$$VdP = SdT + Nd\mu. \tag{2.22}$$

In terms of energy, entropy and number densities defined as $\epsilon \equiv E/V$, $s \equiv S/V$, and $n \equiv N/V$ respectively, the Euler's relation, Eq. (2.21) and Gibbs-Duhem relation, Eq. (2.22), reduce to

$$\epsilon = -P + Ts + \mu n \tag{2.23}$$

$$dP = s\, dT + n\, d\mu. \tag{2.24}$$

Differentiating Eq.(2.23) and using Eq. (2.24), we obtain the relation analogous to first law of thermodynamics

$$d\epsilon = Tds + \mu\, dn \quad \Rightarrow \quad ds = \frac{1}{T}\, d\epsilon - \frac{\mu}{T}\, dn. \tag{2.25}$$

It is important to note that all the densities defined above (ϵ, s, n) are intensive quantities.

The equilibrium state of a system is defined as a stationary state where the extensive and intensive variables of the system do not change.

We know from the second law of thermodynamics that the entropy of an isolated thermodynamic system must either increase or remain constant. Hence, if a thermodynamic system is in equilibrium, the entropy of the system being an extensive variable, must remain constant. On the other hand, for a system that is out of equilibrium, the entropy must always increase. for a more detailed review, see Ref. [33].

2.5.1 Thermodynamic Consistency

The thermodynamics is characterised by four general thermodynamic laws, which describe the universal behaviour of any system irrespective of the details of microscopic mechanisms [30]. We know that the Boltzmann entropy is given by (for complete description (see Appendix (A)) :

$$S^B = -g\sum_i [f_i \ln f_i - f_i] \tag{2.26}$$

Where g is the degeneracy factor and the Tsallis entropy is given by:

$$S_T^B = -g\sum_i [f_i^q \ln_q x - f_i]$$

$$f_i^q = \left[1 + (q-1)\frac{E-\mu}{T}\right]^{-\frac{q}{q-1}} \tag{2.27}$$

In a more generalized way we can express it as:
Partition function for Boltzmann is the first and second laws of thermodynamics lead to the following two differential relations as in Eq. (2.23), (2.24), [34]:

$$d\epsilon = Tds + \mu dn, \tag{2.28}$$

$$dP = sdT + nd\mu. \tag{2.29}$$

where $\epsilon = E/V$, $s = S/V$ and $n = N/V$ are the energy, entropy and particle densities, respectively. Thermodynamic consistency requires that the following relations be satisfied

$$T = \left.\frac{\partial \epsilon}{\partial s}\right|_n, \tag{2.30}$$

$$\mu = \left.\frac{\partial \epsilon}{\partial n}\right|_s, \tag{2.31}$$

$$n = \left.\frac{\partial P}{\partial \mu}\right|_T, \tag{2.32}$$

$$s = \left.\frac{\partial P}{\partial T}\right|_\mu. \tag{2.33}$$

By maximizing the entropy we can obtain expression for particle density, energy density and pressure. All are given by corresponding integrals over Tsallis distributions and the derivatives have to reproduce the corresponding physical quantities, *e.g.* for Tsallis-Boltzmann one has:

$$n_T^B = g\int \frac{d^3p}{(2\pi)^3}\left[1+(q-1)\frac{E-\mu}{T}\right]^{-\frac{q}{q-1}}, \tag{2.34}$$

$$\epsilon_T^B = g\int \frac{d^3p}{(2\pi)^3}E\left[1+(q-1)\frac{E-\mu}{T}\right]^{-\frac{q}{q-1}}, \tag{2.35}$$

$$P_T^B = g\int \frac{d^3p}{(2\pi)^3}\frac{p^2}{3E}\left[1+(q-1)\frac{E-\mu}{T}\right]^{-\frac{q}{q-1}}. \tag{2.36}$$

These expressions should satisfy with the basic thermodynamic relations (2.30), (2.31),(2.32), and (2.33) for consistency, it has to be shown that

$$n_T^B = \frac{\partial P_T^B}{\partial \mu} \tag{2.37}$$

Let us consider

$$P = \frac{-E+TS+\mu N}{V}, \tag{2.38}$$

and take the partial derivative with respect to μ in order to check for thermodynamic consistency, it leads to

$$
\begin{aligned}
\left.\frac{\partial P}{\partial \mu}\right|_T &= \frac{1}{V}\left[-\frac{\partial E}{\partial \mu}+T\frac{\partial S}{\partial \mu}+N+\mu\frac{\partial N}{\partial \mu}\right], \\
&= \frac{1}{V}\left[N+\sum_i -\frac{T}{q-1}\left(1+(q-1)\frac{E_i-\mu}{T}\right)\frac{\partial f_i^q}{\partial \mu}\right. \\
&\quad \left. +\frac{Tq(1-f_i)^{q-1}}{q-1}\frac{\partial f_i}{\partial \mu}\right],
\end{aligned} \tag{2.39}
$$

then,

$$
\begin{aligned}
\frac{\partial f_i^q}{\partial \mu} &= \frac{qf_i^{q+1}}{T}\left[1+(q-1)\frac{E_i-\mu}{T}\right]^{-1+\frac{1}{1-q}}, \\
\frac{\partial f_i}{\partial \mu} &= \frac{f_i^2}{T}\left[1+(q-1)\frac{E_i-\mu}{T}\right]^{-1+\frac{1}{1-q}},
\end{aligned}
$$

and

$$
(1-f_i)^{q-1} = f_i^{q-1}\left[1+\frac{(q-1)(E_i-\mu)}{T}\right].
$$

Putting this into Eq. (2.39), yields

$$
\left.\frac{\partial P}{\partial \mu}\right|_T = n, \tag{2.40}
$$

It proves thermodynamic consistency (2.32).

Then by the relation in Eq. (2.30) can be written as:

$$
\begin{aligned}
\left.\frac{\partial E}{\partial S}\right|_n &= \frac{\frac{\partial E}{\partial T}dT+\frac{\partial E}{\partial \mu}d\mu}{\frac{\partial S}{\partial T}dT+\frac{\partial S}{\partial \mu}d\mu}, \\
&= \frac{\frac{\partial E}{\partial T}+\frac{\partial E}{\partial \mu}\frac{d\mu}{dT}}{\frac{\partial S}{\partial T}+\frac{\partial S}{\partial \mu}\frac{d\mu}{dT}},
\end{aligned} \tag{2.41}
$$

n is kept fixed

$$
dn = \frac{\partial n}{\partial T}dT+\frac{\partial n}{\partial \mu}d\mu = 0,
$$

leading to

$$
\frac{d\mu}{dT} = -\frac{\frac{\partial n}{\partial T}}{\frac{\partial n}{\partial \mu}}. \tag{2.42}
$$

Hence we rewrite (2.41) and (2.42) in terms of the following expressions:

$$\frac{\partial E}{\partial T} = \sum_i qE_i f_i^{q-1}\frac{\partial f_i}{\partial T},$$

$$\frac{\partial E}{\partial \mu} = \sum_i qE_i f_i^{q-1}\frac{\partial f_i}{\partial \mu},$$

$$\frac{\partial S}{\partial T} = \sum_i q\left[\frac{-f_i^{q-1}+(1-f_i)^{q-1}}{q-1}\right]\frac{\partial f_i}{\partial T},$$

$$\frac{\partial S}{\partial \mu} = \sum_i q\left[\frac{-f_i^{q-1}+(1-f_i)^{q-1}}{q-1}\right]\frac{\partial f_i}{\partial \mu},$$

$$\frac{\partial n}{\partial T} = \frac{1}{V}\left[\sum_i q f_i^{q-1}\frac{\partial f_i}{\partial T}\right],$$

and

$$\frac{\partial n}{\partial \mu} = \frac{1}{V}\left[\sum_i q f_i^{q-1}\frac{\partial f_i}{\partial \mu}\right].$$

Putting the above relations into Eq. (2.41), the numerator of Eq. (2.41) becomes

$$\begin{aligned}\frac{\partial E}{\partial T} + \frac{\partial E}{\partial \mu}\frac{d\mu}{dT} &= \sum_i qE_i f_i^{q-1}\frac{\partial f_i}{\partial T} \\ &\quad -\frac{\displaystyle\sum_{i,j} q^2 E_j\left(f_i f_j\right)^{q-1}\frac{\partial f_j}{\partial \mu}\frac{\partial f_i}{\partial T}}{\displaystyle\sum_j q f_j^{q-1}\frac{\partial f_j}{\partial \mu}}, \\ &= \frac{\displaystyle\sum_{i,j} qE_i\left(f_i f_j\right)^{q-1} C_{ij}}{\displaystyle\sum_j f_j^{q-1}\frac{\partial f_j}{\partial \mu}}.\end{aligned} \tag{2.43}$$

Where C_{ij}

$$C_{ij} \equiv \left(f_i f_j\right)^{q-1}\left[\frac{\partial f_i}{\partial T}\frac{\partial f_j}{\partial \mu} - \frac{\partial f_j}{\partial T}\frac{\partial f_i}{\partial \mu}\right], \tag{2.44}$$

Hence by Eq. (2.41)

$$\frac{\partial S}{\partial T}+\frac{\partial S}{\partial \mu}\frac{d\mu}{dT} = \frac{q\sum_{i,j}\left[-f_i^{q-1}+(1-f_i)^{q-1}\right]f_j^{q-1}C_{i,j}}{(q-1)\sum_j f_j^{q-1}\frac{\partial f_j}{\partial \mu}},$$
$$= \frac{q\sum_{i,j}(E_i-\mu)\,(f_if_j)^{q-1}\,C_{i,j}}{T\sum_j f_j^{q-1}\frac{\partial f_j}{\partial \mu}}, \tag{2.45}$$

where

$$\frac{-f_i^{q-1}+(1-f_i)^{q-1}}{q-1}=\frac{(E_i-\mu)}{T}f_i^{q-1},$$

hence, by substituting Eqs. (2.43) and (2.45) in to Eq. (2.41),

$$\left.\frac{\partial E}{\partial S}\right|_n = T\frac{\sum_{i,j}E_iC_{ij}}{\sum_{i,j}(E_i-\mu)C_{ij}}, \tag{2.46}$$

since $\sum_{i,j}C_{ij}=0$, this finally leads to the desired result

$$\left.\frac{\partial E}{\partial S}\right|_n = T. \tag{2.47}$$

Hence thermodynamic consistency is satisfied.

It is shown that temperature and pressure within the Tsallis formalism for non-extensive statistics lead to expressions which satisfy consistency with the first and second laws of thermodynamics. Hence we showed explicitly that, the Tsallis statistics is thermodynamically consistent.

2.6 Different forms of Tsallis Distribution Function

Extensive and non-extensive statistical approaches have been used to characterize particle spectra in terms of thermodynamic variables. Extensive statistics assume thermal and chemical equilibrium of the system at hadronic phase which lead to an exponential distribution of the particle spectra. In experiments, the particle spectra show a power-law behavior at high-$\mathrm{p_T}$. This behavior is reproduced by the non-extensive approach with an additional parameter. In recent times, the Tsallis [38] statistical approach is widely used to describe the particle spectra obtained in high-energy collisions with only two parameters; the temperature T and q, known as non-extensivity parameter which is a measure of temperature fluctuations or degree of non-equilibrium in the system. The Tsallis distribution gives an excellent description of $\mathrm{p_T}$ spectra of all identified mesons measured in $p+p$ collisions at $\sqrt{\mathrm{s_{NN}}}$=200 GeV [20, 46]. Here we will quantify a cross connection between different versions of Tsallis distribution. In the framework of Tsallis statistics, the distribution function is,

$$f(E,q) = [1 + (q-1)\frac{E-\mu}{T}]^{-\frac{1}{q-1}} \tag{2.48}$$

The expression for the average number as in Eq. (2.34) of particles using the Tsallis expression is given by,

$$N = gV \int \frac{d^3p}{(2\pi)^3} \left[1 + (q-1)\frac{E-\mu}{T}\right]^{-\frac{q}{q-1}} \tag{2.49}$$

Using the fact that $E = m_T \cosh y$ and $p_z = m_T \sinh y$

$$N = gV \int \frac{dp_T d\phi dy p_T m_T \cosh y}{(2\pi)^3} \left[1 + \frac{(q-1)(m_T \cosh y - \mu)}{T}\right]^{-q/q-1}, \tag{2.50}$$

where T is the temperature and μ is the chemical potential, V is the volume and g is the degeneracy factor. For the Tsallis distribution the transverse momentum distribution can be written as,

$$\frac{d^3N}{d^3p} = \frac{gV}{(2\pi)^3}\left[1+(q-1)\frac{E-\mu}{T}\right]^{-q/(q-1)} \tag{2.51}$$

in terms of transverse momentum ($\mathrm{p_T}$), transverse mass ($m_T = \sqrt{p_T^2+m^2}$), and rapidity (y). Let us consider it as Type-A distribution.

$$E\frac{d^3N}{dp^3} = gV\frac{m_T\cosh y}{(2\pi)^3}[1+(q-1)\frac{m_T\cosh y-\mu}{T}]^{-\frac{q}{q-1}} \tag{2.52}$$

or,

$$\frac{dN}{dp_T dy} = gV\frac{p_T m_T\cosh y}{(2\pi)^2}\left[1+\frac{(q-1)m_T\cosh y-\mu}{T}\right]^{q/1-q} \tag{2.53}$$

Let us consider equation (2.52) Type-B distribution. At mid-rapidity(y=0), and zero chemical potential(μ=0) it relates to [54],

$$\begin{aligned} \left.\frac{d^2N}{dp_T\ dy}\right|_{y=0} &= gV\frac{p_T m_T}{(2\pi)^2}\left[1+(q-1)\frac{m_T}{T}\right]^{q/(1-q)} \\ E\frac{d^3N}{dp^3} &= gV\frac{m_T}{(2\pi)^3}[1+(q-1)\frac{m_T}{T}]^{q/(1-q)} \end{aligned} \tag{2.54}$$

As q→1 it reduces to the standard Boltzmann distribution,

$$\lim_{q\to 1}\frac{d^2N}{dp_T\ dy} = gV\frac{p_T m_T\cosh y}{(2\pi)^2}\exp\left(-\frac{m_T\cosh y-\mu}{T}\right) \tag{2.55}$$

The parameterization given in (2.53) is so close to the one used by the STAR, PHENIX, ALICE and CMS experiments.

$$\frac{d^2N}{dp_T\, dy} = p_T\frac{dN}{dy}\frac{(n-1)(n-2)}{nC(nC+m_0(n-2))}\left[1+\frac{m_T-m_0}{nC}\right]^{-n} \tag{2.56}$$

or we can write it as,

$$\begin{aligned} E\frac{d^3N}{dp^3} &= \frac{1}{2\pi p_T}\frac{d^2N}{dydp_T} \\ &= \frac{dN}{dy}\frac{(n-1)(n-2)}{2\pi nC[nC+m(n-2))]}(1+\frac{m_T-m}{nC})^{-n} \end{aligned} \tag{2.57}$$

where $n \rightarrow \frac{q}{q-1}$, $nC \rightarrow \frac{T+m_0(q-1)}{q-1}$, $m_T = \sqrt{p_T^2 + m^2}$ is the transverse mass. m, $\frac{dN}{dy}$, n and C are fitting parameters. Let us consider equation (2.57) as Type-A distribution. Hence this equation can also be understood as an interpolation between low transverse momenta and high transverse momenta [55]. By using Eqn. (2.57), when $p_T >> m$ (ignoring m) we can ignore m, one gets [56],

$$E\frac{d^3N}{dp^3} \propto p_T^{-n}$$

which is a power-law type distribution. When $p_T << m$ we get,

$$\begin{aligned} m_T - m &= \frac{p_T^2}{2m} = E_T^{classical} \\ E\frac{d^3N}{dp^3} &\propto e^{\frac{-E_T^{classical}}{C}} \end{aligned} \tag{2.58}$$

This is a Boltzmann-type thermal distribution. The parameter C in (2.57) plays same role as temperature T. Now we obtain the simpler form of (2.57)

$$\begin{aligned} E\frac{d^3N}{dp^3} &= A(1 + \frac{m_T - m}{nT})^{-n} \\ E\frac{d^3N}{dp^3} &= A(1 + \frac{E_T}{nT})^{-n} \end{aligned} \tag{2.59}$$

As it is seen that Equations (2.59) and (2.54) seem very similar but there is some difference between them, $i.e$ there is no direct match between n and q in Equations (2.59) (2.54). But to find relation between them, let's assume $p_T >> m$, then by (2.54) we can get;

$$E\frac{d^3N}{dp^3} \propto p_T^{-\frac{1}{q-1}} \tag{2.60}$$

Therefore relation between n and q is

$$n = \frac{q}{q-1} \tag{2.61}$$

Another treatment to find the relation between n and q can be found in ref [58]. Now it is noted that the cross connection between Type-A and

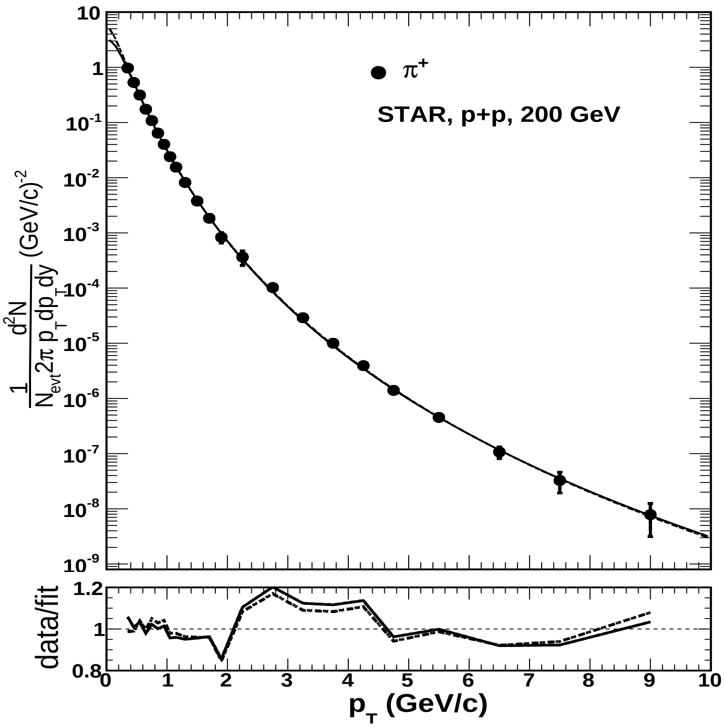

Figure 2.2. Fitting results for Eqs. (2.52) (2.57) for π^+ in p+p collisions at $\sqrt{=}200$ GeV. The solid line, dashed line, refer to Eqs. (2.52) (2.57) respectively. The ratios of data/fit are shown at the bottom [56]. Data are taken from STAR [43]

Type-B Tsallis distribution is that they can reproduce the particle spectra in p+p collisions very well but Type-B gives lower temperatures than ones given by Type-A as in [56].

Chapter 3

Nuclear Modification Factor R_{AA} using Non-Extensive Statistics

High momentum suppression of light and heavy flavours is considered to be an excellent probe of jet-medium interactions in QCD matter created at RHIC and LHC. Utilizing this tool requires accurate suppression predictions for different experiments, probes and experimental conditions, and their unbiased comparison with experimental data.

Relativistic heavy-ion collisions are the means to produce the quark gluon plasma in laboratory and study its properties. Hadrons, which are abundantly produced in these collisions, are one of the main tools to study the properties of this hot/dense medium produced. For these hadrons we are using Non-extensive statistics. By using it we develope a transport model for R_{AA} estimation.

As we know one of the main tasks of the theory is to link experimental observables to the different phases and manifestations of the QCD matter. To achieve this goal, a detailed understanding of the dynamics of heavy-ion reactions is essential. This is facilitated by transport theory which helps to interpret or predict the quantitative features of heavy ion reactions. It is particularly well suited for the non-equilibrium situation, freeze-out as well as for collective dynamics. Transport models attempt to describe the full time-evolution from the initial state of the heavy ion reaction up to the freeze-out of all initial and produced particles after the reaction.

3.1 Nuclear Modification Factor Overview In Light Flavour and Heavy Flavour

In order to characterize the quark gluon plasma (QGP), we can study the characteristics of produced mesons containing at least one heavy quark (c or b, like $c\bar{c} = J/\Psi$, $b\bar{b} = \Upsilon$). Comparing their final distribution to the initial one tells us about certain properties of the QGP, such as its pressure and density.

Heavy quarks (charm and beauty) provide sensitive probes of the heavy-ion collision dynamics at both short and long timescales. On one hand, heavy-flavour production is an intrinsically perturbative phenomenon which involves large momentum transfer due to the large mass of the quarks ($m_c \approx 1.5$ GeV/c^2 and $m_b \approx 5$ GeV/c^2) and, thus, takes place on a short timescale, smaller than the formation time of the QGP. On the other hand, the long lifetime of charm and beauty quarks allows them to live through the thermalization phase of the plasma and to possibly interact with the constituents of the medium.

For all of this and also as by the requirement of our model we need the information about the transverse momentum of hadrons. The hadron transverse momentum spectra give insight of particle production mechanisms, bulk properties and evolution of system. Along with this, the quark contents of hadrons also play a major role in understanding the interactions and behavior of different types quarks inside the medium such as Light quark and Heavy quark. The heavy quark production and their interaction with the strongly interacting medium, formed in high-energy heavy-ion collisions, is one of the topic of our consideration. Given their large masses charm and beauty quarks are produced in hard-scattering processes with large momentum transfer. Partons traversing the hot-dense medium produced in heavy-ion collisions suffer significant energy loss which results in the modification of fragmentation functions and softening of particle spectra. This modification is quantified by "Nuclear Modification Factor"

(R_{AA}), which is defined as the ratio of the yield in heavy-ion collision (Au-Au, Cu-Cu or Pb-Pb) to the yield in "p+p" collisions scaled by the number of binary collisions. The deviation of R_{AA} from unity is a manifestation of the medium effects.

$$R_{AA} = \frac{1}{N_{coll}} \frac{d^2N_{AA}/p_T dy dp_T}{d^2N_{pp}/p_T dy dp_T}.$$

where the numerator is the of particle production in heavy-ion collisions, measured as a function of p_T and rapidity (y) and $d^2N_{PP}/p_T dy dp_T$ is the yeild of the same process in $p+p$ collisions and N_{coll} is the number of nucleon-nucleon collisions in the system. Heavy quarks are produced primarily at early stages of heavy-ion collisions due to their large masses, and therefore they carry information about the pre-thermalization properties of the quark gluon plasma produced in such collisions. Our model to calculate R_{AA} is quite different from this method. We have used the Non-Extensive statistical mechanics to study the behaviour of the nuclear matter created in the heavy-ion collision. Our approach is related to transport equation, i.e. Boltzmann Transport Equation.

3.1.1 Simplistic Boltzmann Transport Equation (BTE) and Relaxation Time Approximation (RTA)

The Boltzmann Transport Equation describes the statistical behaviour of a thermodynamic system not in thermodynamic equilibrium. Boltzmann equation is often used in a more general sense and it refers to any kinetic equation that describes the change of a macroscopic quantity in a thermodynamic system. Specifically non-equilibrium statistical mechanics, the Boltzmann equation or Boltzmann transport equation (BTE) describes the statistical behaviour of a thermodynamic system not in thermodynamic equilibrium. It was devised by Ludwig Boltzmann in 1872. The classic example is a fluid with temperature gradients in space causing heat to flow from hotter regions to colder ones, by the random (and biased) transport of particles. In the modern literature the term Boltzmann equation is often used in a more general sense and refers to any kinetic equation that describes the change of a macroscopic quantity in a thermodynamic system, such as energy, charge or particle number. Consider particles described by f, where f is a function of position, momentum and time.

The total differential of f is:

$$\begin{aligned} df &= \frac{\partial f}{\partial t}dt + \left(\frac{\partial f}{\partial x}dx + \frac{\partial f}{\partial y}dy + \frac{\partial f}{\partial z}dz\right) + \left(\frac{\partial f}{\partial p_x}dp_x + \frac{\partial f}{\partial p_y}dp_y + \frac{\partial f}{\partial p_z}dp_z\right) \\ &= \frac{\partial f}{\partial t}dt + \nabla f \cdot d\mathbf{r} + \frac{\partial f}{\partial \mathbf{p}} \cdot d\mathbf{p} \\ &= \frac{\partial f}{\partial t}dt + \nabla f \cdot \frac{\mathbf{p}dt}{m} + \frac{\partial f}{\partial \mathbf{p}} \cdot F dt \end{aligned} \tag{3.1}$$

Dividing Eq. (3.1) by dt we get

$$\frac{df(x,p,t)}{dt} = \frac{\partial f}{\partial t} + \vec{v}\nabla_x f + F.\nabla_p f \tag{3.2}$$

Assuming the system is homogeneous and no external force is on the system, the 2nd and 3rd term of the above equation goes to zero. So Eq. 3.2 becomes,

$$\frac{df(x,p,t)}{dt} = \frac{\partial f}{\partial t} \tag{3.3}$$

In this scenario it is possible to interpret the collision terms as due to drag forces and diffusion induced by random collisions. In more precise way we can recapitulate things as, in initial stage of collision when energy density is very high, there is a production of heavy particles like charm quark, means all heavy particles like J/Ψ, Υ etc. Now after this lighter particles start their formation because there is not much energy density. Now when medium is formed after the collision some of them may travel through the medium(QGP)such that they loose some energy passing through medium.

So, inside the medium some high energy particles due to interaction come to the the low energy $\mathrm{p_T}$ because of energy loss and some low energy particles due to energy gain come to high energy $\mathrm{p_T}$. There will be something like loosing and gaining in this $\mathrm{p_T}$ range. So we need the information about the heavy quarks(Υ J/Ψ), etc & also information about the medium. This is generally dictated by pQCD because the $\mathrm{p_T}$ is very high in the begining. So these are called probes, because by all of this we can understand, "How the medium is behaving and energy loss here is related to drag and diffusion like transport coefficients of the medium".

By all this phenomena, we can quantify that, "How the medium is behaving". So these particles are nothing but some probe particles used to quantify the nuclear medium effect. So here we can define Nuclear Modification Factor (R_{AA}) as;

$$R_{AA} = \frac{f_{final}}{f_{initial}} \tag{3.4}$$

where, $f_{initial}$ is the initial distribution of the particles during the formation and f_{final} is the distribution of the particles after the interaction with medium.

Evolution of a thermodynamic system which is not in thermodynamic equilibrium is governedby Boltzmann transport equation, which is given by (3.2)

In relaxation time approximation, for deviations of distribution function f from the equilibrium state f_{eq}, by Eqn. 3.3 collision term is expressed as

$$\frac{\partial f}{\partial t} = -\frac{f - f_{eq}}{\tau_R} \tag{3.5}$$

Where τ_R is relaxation time, which is the time taken by a non-equilibrium system to become a equilibrium system. Putting back in Eq. 3.3

$$\frac{df(x,p,t)}{dt} = -\frac{f - f_{eq}}{\tau_R} \tag{3.6}$$

Solving the above equation in view of initial conditions,

$$f_{final} = f_{eq} + (f_{initial} - f_{eq})e^{-\frac{t_F}{\tau_R}} \tag{3.7}$$

The final heavy-quark (HQ) spectra may therefore encode a "memory" of the interaction history throughout the evolving fireball, by operating in between the limits of thermalization and free streaming. Now, the nuclear modification factor is given by

$$R_{AA} = \frac{f_{fin}}{fin} = \frac{f_{eq}}{f_{in}} + \left(1 - \frac{f_{eq}}{f_{in}}\right) e^{\frac{-t_F}{\tau_R}} \tag{3.8}$$

where Boltzmann equilibrium distribution is given by:

$$f_{eq} = \frac{gV}{(2\pi)^2} p_T m_T e^{-\frac{m_T}{T_{eq}}} \tag{3.9}$$

As the system is in non-equilibrium state, a thermodynamically consistent non-extensive distribution function is given by:

$$f_{initial} = \frac{gV}{(2\pi)^2} p_T m_T \left[1 + (q-1)\frac{m_T}{T}\right]^{-\frac{q}{q-1}}. \tag{3.10}$$

Here, V is the system volume, $m_{\mathrm{T}} = \sqrt{p_T^2 + m^2}$ is the transverse mass and q is called the non-extensive parameter which measures the degree of deviation from equilibrium. Using Eqs. 3.9 and 3.10(both for mid-rapidity and for zero chemical potential) nuclear modification factor can be calculated.

3.1.2 Tsallis-Boltzmann Distribution for R_{AA} in $\mathcal{O}(q-1)$

Here heavy quark because quarkonia of heavy quark-antiquark bound states are promising probes for the QGP created in relativistic heavy-ion collisions. Many studies have been carried out in recent years. These include experimental measurements of its yield in heavy ion collisions at both the

Relativistic Heavy Ion Collider (RHIC) and the Large Hadron Collider (LHC), as well as theoretical studies based on various models. These studies have indicated that a quantitative description of quarkonium production in these collisions requires the understanding of its interactions in both the produced QGP and study of the initial and final distribution. Heavy-flavor particles are believed to provide valuable probes of the medium produced in ultra-relativistic collisions of heavy nuclei. Taylor series expansion of the (3.10) Tsallis distribution for $\mathcal{O}\left\{(q-1)\right\}\mathcal{O}\left\{(q-1)^2\right\}$ is showing here using it we will calculate the Nuclear Modification Factor:

$$\begin{aligned} & \left[1+(q-1)\frac{E-\mu}{T}\right]^{-\frac{q}{q-1}} \\ \simeq\ & \mathrm{e}^{-\frac{E-\mu}{T}}\left\{1+(q-1)\frac{1}{2}\frac{E-\mu}{T}\left(-2+\frac{E-\mu}{T}\right)\right. \\ +\ & \frac{(q-1)^2}{2!}\frac{1}{12}\left[\frac{E-\mu}{T}\right]^2\left[24-20\frac{E-\mu}{T}+3\left(\frac{E-\mu}{T}\right)^2\right] \\ +\ & \mathcal{O}\left\{(q-1)^3\right\} \\ +\ & \left. ...\right\} \end{aligned} \tag{3.11}$$

in (3.11) if $\mu = 0$ then the initial distribution f_{in} for $\mathcal{O}(q-1)$ will be

$$f_{in} = e^{-\frac{E}{T}}\left\{1+\left(\frac{q-1}{2}\right)\left(\frac{E}{T}\right)\left(-2+\frac{E}{T}\right)\right\} \tag{3.12}$$

and f_{eq} will be

$$f_{eq} = e^{-\beta E}, \tag{3.13}$$

where $E = m_T \cosh\eta$ and $m_T = \sqrt{m^2+p_T^2}$
Putting values of equation (3.12) and equation (3.13) in equation (3.8) and using $\mu = 0$ and $\eta = 0$ we get,

$$R_{AA} = \frac{1}{1+\frac{(q-1)}{2}\frac{m_T}{T}(-2+\frac{m_T}{T})} + \left[1-\frac{1}{1+\frac{(q-1)}{2}\frac{m_T}{T}(-2+\frac{m_T}{T})}\right]e^{\frac{-t_F}{\tau_R}} \tag{3.14}$$

Here t_F is freeze-out time & τ_R is the relaxation time. For J/Ψ particle the values of $t_F = 0.8$, $\tau_R = 0.2$ are chosen to be and mass $m = 3.096$ GeV/c^2.

Here we plot our function R_{AA} v_s $\mathrm{p_T}$. To identify some interesting thing we have to do the same procedure for different statistics. Only after that we can came on a conclusion.

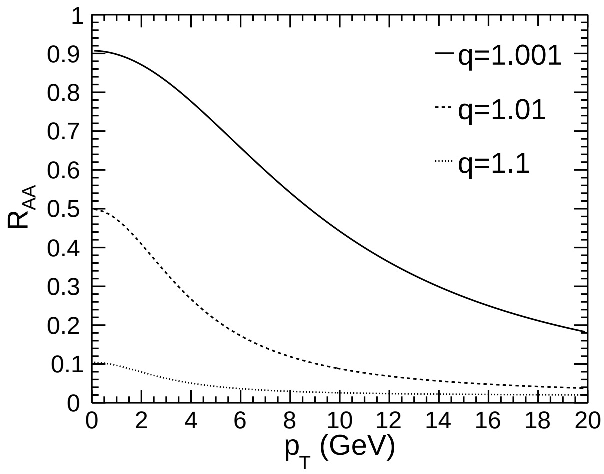

Figure 3.1. Nuclear modification factor versus $\mathrm{p_T}$ graph for different values of non-extensive parameter using Tsallis Boltzmann Distribution with $O(q-1)$.

3.1.3 Tsallis-Boltzmann Distribution for R_{AA} in $\mathcal{O}(q-1)^2$

Now by using the expansion of eq (3.11) up to second order we get:

$$f_{in} = e^{\frac{m_T}{T}} \left[1 + \left(\frac{q-1}{2}\right)\left(\frac{m_T}{T}\right)\left(-2 + \frac{m_T}{T}\right)\right] + \frac{(q-1^2)}{2!}\frac{1}{12}\left(\frac{m_T}{T}\right)^2 \left[\left\{24 - 20\frac{m_T}{T} + 3\left(\frac{m_T}{T}\right)^2\right\}\right] \quad (3.15)$$

Putting equation (3.15) and equation (3.13) in (3.8)

$$R_{AA} = \frac{1}{1 + \frac{(q-1)}{2}\frac{m_T}{T}\left(-2 + \frac{m_T}{T}\right) + \frac{(q-1)}{2!}^2\frac{1}{12}\left(\frac{m_T}{T}\right)^2\left(24 - 20\frac{m_T}{T} + 3\left(\frac{m_T}{T}\right)^2\right)}$$
$$\left[1 - \frac{1}{1 + \frac{(q-1)}{2}\frac{m_T}{T}\left(-2 + \frac{m_T}{T}\right) + \frac{(q-1)}{2!}^2\frac{1}{12}\left(\frac{m_T}{T}\right)^2\left(24 - 20\frac{m_T}{T} + 3\left(\frac{m_T}{T}\right)^2\right)}\right] e^{\frac{-t_F}{\tau_R}}$$

This is the Eqn. (3.16) is final expression of R_{AA} for $\mathcal{O}(q-1)^2$. Hence we can conclude that at $q=1$ there no effect of order & suppression has the same magnitude as at the $q=1$ for $\mathcal{O}(q-1)$.

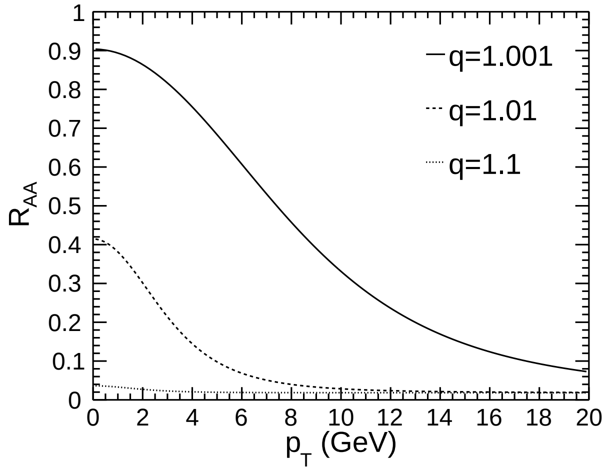

Figure 3.2. Nuclear modification factor versus $\mathrm{p_T}$ graph for different values of non-extensive parameter using Tsallis Boltzmann Distribution with $O(q-1)^2$ [62].

3.1.4 Tsallis Bose-Einstein Distribution for R_{AA} in $\mathcal{O}(q-1)$

The Tsallis Bose-Einstein distribution is,

$$f_T^{BE} = \left((x\Phi+1)^{1/2}-1\right)^{-x-1}, \tag{3.16}$$

where $\Phi = \frac{E-\mu}{T}$, $x=(q-1)$.

After Taylor expansion in up to $\mathcal{O}(q-1)$ we get the initial distribution

$$f_T^{BE} = \frac{1}{e^{\Phi}-1} + \frac{xe^{\Phi}\Phi^2 - 2(e^{\Phi}-1)\log(e^{\Phi}-1)}{2(e^{\Phi}-1)^2} \tag{3.17}$$

$$f_{eq} = \frac{1}{e^{\Phi}-1} \tag{3.18}$$

$$f_{in} = f_T^{BE} \tag{3.19}$$

Using (3.17), (3.18), (3.19) in equation (3.8) we get,

$$R_{AA} = \frac{1}{1+\frac{xe^{\Phi}\Phi^2-2(e^{\Phi}-1)\log(e^{\Phi}-1)}{2(e^{\Phi}-1)}}\left[\frac{1}{1+\frac{xe^{\Phi}\Phi^2-2(e^{\Phi}-1)\log(e^{\Phi}-1)}{2(e^{\Phi}-1)}}\right]e^{\frac{-t_F}{\tau_R}} \quad (3.20)$$

Here t_F is freeze-out time & τ_R is the relaxation time. For J/Ψ particle the values of t_F, τ_R are chosen to be and mass $m = 3.096$ GeV$/c^2$. Hence we can conclude that at $q = 1$ there no effect of order & suppression has the same magnitude as at the $q = 1$ for $\mathcal{O}(q-1)$ hence the model is statistically independent. At $q = 1$ it follows same as in Boltzmann.

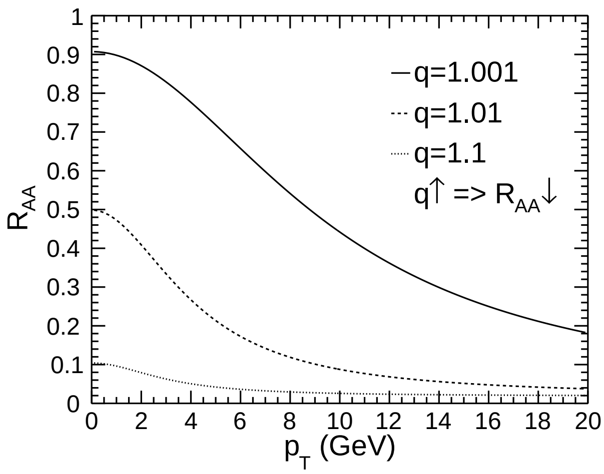

Figure 3.3. Nuclear modification factor versus $\mathrm{p_T}$ graph for different values of non-extensive parameter using Tsallis Bose-Einstein Distribution with $O(q-1)$.

3.1.5 Tsallis Bose-Einstein Distribution for R_{AA} in $\mathcal{O}(q-1)^2$

After the Taylor expansion upto $\mathcal{O}(q-1)^2$ we get the initial distribution,

$$f_T^{BE} = \frac{1}{e^{\Phi}-1} + \frac{xe^{\Phi}\Phi^2 - 2(e^{\Phi}-1)\log(e^{\Phi}-1)}{2(e^{\Phi}-1)^2}$$
$$+\frac{x^2}{2!}\frac{3(e^{\Phi}\Phi^2-2(e^{\Phi}-1)\log(e^{\Phi}-1))^2 - e^{\Phi}\Phi^2(-3\Phi^2-8\Phi+4e^{\Phi}(2\Phi-3)+12)}{12(e^{\Phi}-1)^3}$$

$$f_{in} = f_T^{BE} \quad (3.21)$$

Using equation (3.21), (3.18), in equation (3.8) we get

$$R_{AA} = \frac{1}{1+\frac{xe^{\Phi}\Phi^2-2(e^{\Phi}-1)\log(e^{\Phi}-1)}{2(e^{\Phi}-1)}+A}\left[1-\frac{1}{1+\frac{xe^{\Phi}\Phi^2-2(e^{\Phi}-1)\log(e^{\Phi}-1)}{2(e^{\Phi}-1)}+A}\right]e^{\frac{-t_F}{\tau_R}}$$

This is the Eqn.(3.22) is final expression for R_{AA} for $\mathcal{O}(q-1)^2$. Here t_F is freeze-out time & τ_R is the relaxation time. For J/Ψ particle the values of t_F, τ_R are chosen to be and mass $m = 3.096$ GeV/c^2. Hence we can conclude that at $q = 1$ there no effect of order & suppression has the same magnitude as at the $q = 1$ for $\mathcal{O}(q-1)$ hence the model is statistically independent.

$$A = \frac{x^2}{2!}\frac{3(e^{\Phi}\Phi^2-2(e^{\Phi}-1)\log(e^{\Phi}-1))^2-e^{\Phi}\Phi^2(-3\Phi^2-8\Phi+4e^{\Phi}(2\Phi-3)+12)}{12(e^{\Phi}-1)^2}$$

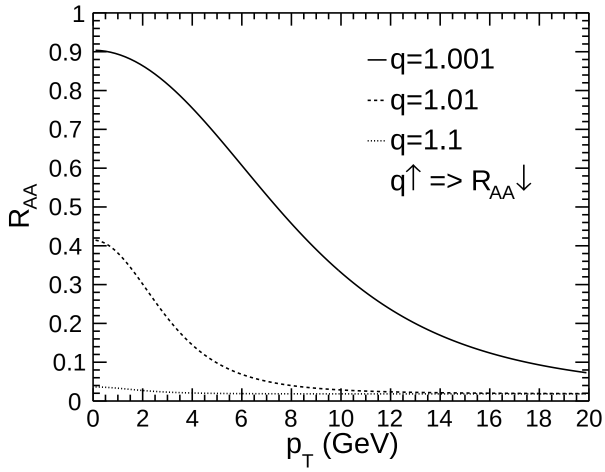

Figure 3.4. Nuclear modification factor versus $\mathrm{p_T}$ graph for different values of non-extensive parameter using Tsallis Bose-Einstein Distribution with $O(q-1)^2$.

3.1.6 Tsallis Fermi-Dirac distribution for R_{AA} in $\mathcal{O}(q-1)$

Tsallis Fermi-Dirac distribution is

$$f_T^{FD} = \left((x\Phi + 1)^{1/2} + 1\right)^{-x-1} \tag{3.22}$$

where $\Phi = \frac{E-\mu}{T}$, $x = (q-1)$ After the Taylor expansion upto $\mathcal{O}(q-1)$ we get the initial distribution,

$$f_T^{FD} = \frac{1}{e^\Phi + 1} + \frac{xe^\Phi\Phi^2 - 2(e^\Phi + 1)\log(e^\Phi + 1)}{2(e^\Phi + 1)^2}$$

$$f_{eq} = \frac{1}{e^\Phi + 1} \tag{3.23}$$

$$f_{in} = f_T^{FD} \tag{3.24}$$

Using equation (3.24), (3.23) in equation (3.8) we get

$$R_{AA} = \frac{1}{1 + \frac{xe^\Phi\Phi^2 - 2(e^\Phi+1)\log(e^\Phi+1)}{2(e^\Phi+1)}}\left[1 - \frac{1}{1 + \frac{xe^\Phi\Phi^2 - 2(e^\Phi+1)\log(e^\Phi+1)}{2(e^\Phi+1)}}\right] e^{\frac{-t_F}{\tau_R}} \tag{3.25}$$

Here t_F is freeze-out time & τ_R is the relaxation time. For *lambda* particle the values of $t_F = 0.8$, $\tau_R = 0.2$ are chosen to be and mass $m = 1.15$ GeV/c^2. Hence we can conclude that at $q = 1$ there no effect of order & suppression has the same magnitude as at the $q = 1$ for $\mathcal{O}(q-1)$ hence the model is statistically independent.

3.1.7 Tsallis Fermi-Dirac distribution for R_{AA} in $\mathcal{O}(q-1)^2$

$$\begin{aligned} f_T^{FD} &= \frac{1}{e^\Phi + 1} + \frac{xe^\Phi\Phi^2 - 2(e^\Phi + 1)\log(e^\Phi + 1)}{2(e^\Phi + 1)^2} \\ &+ \frac{x^2}{2!}\frac{3(e^\Phi\Phi^2 - 2(e^\Phi + 1)\log(e^\Phi + 1))^2 - e^\Phi\Phi^2(-3\Phi^2 + 8\Phi + 4e^\Phi(2\Phi - 3) - 12)}{12(e^\Phi + 1)^3} \end{aligned}$$

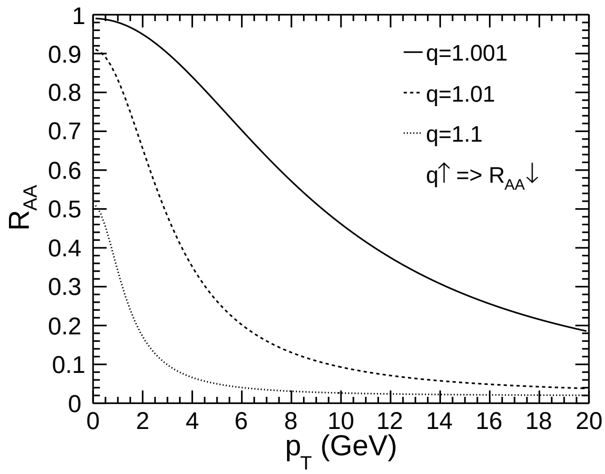

Figure 3.5. Nuclear modification factor versus $\mathrm{p_T}$ graph for different values of non-extensive parameter using Tsallis Fermi-Dirac Distribution with $O(q-1)$.

$$f_{eq} = \frac{1}{e^{\Phi}+1} \tag{3.26}$$

$$f_{in} = f_T^{FD} \tag{3.27}$$

Using equation (3.26) (3.27) in (3.8)

$$R_{AA} = \frac{1}{1+\frac{xe^{\Phi}\Phi^2-2(e^{\Phi}-1)\log(e^{\Phi}+1)}{2(e^{\Phi}+1)}+C}\left[1-\frac{1}{1+\frac{xe^{\Phi}\Phi^2-2(e^{\Phi}+1)\log(e^{\Phi}+1)}{2(e^{\Phi}+1)}+C}\right]e^{\frac{-t_F}{\tau_R}}$$

This Eqn (3.28) is the Tsallis-FD for R_{AA} $\mathcal{O}(q-1)^2$. Here t_F is freeze-out time & τ_R is the relaxation time. For *lambda* particle the values of $t_F = 0.8$, $\tau_R = 0.2$ are chosen to be and mass $m = 1.15$ GeV/c^2. Hence we can conclude that at $q = 1$ there no effect of order & suppression has the same magnitude as at the $q = 1$ for $\mathcal{O}(q-1)$ hence the model is statistically independent.

$$C = \frac{x^2}{2!}\frac{3(e^{\Phi}\Phi^2-2(e^{\Phi}+1)\log(e^{\Phi}+1))^2 - e^{\Phi}\Phi^2(-3\Phi^2+8\Phi+4e^{\Phi}(2\Phi-3)-12)}{12(e^{\Phi}+1)^2}$$

As we know both initial and final state effects are expected to enter in the production and propagation of heavy quarks, respectively; consequently, they are information-rich probes. As these probes containing information about the evolution of the medium and also,"How the medium is behaving

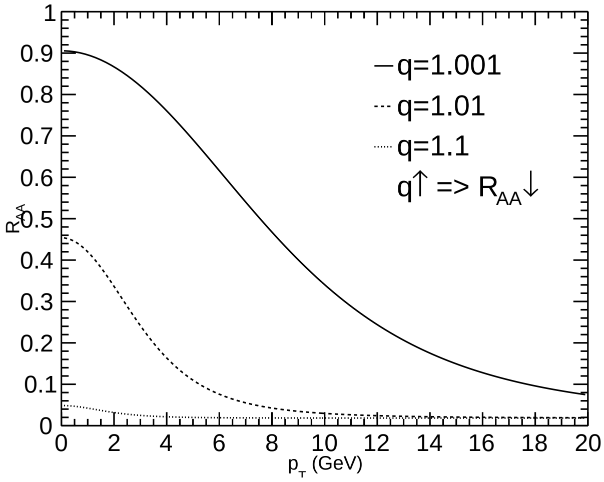

Figure 3.6. Nuclear modification factor versus $\mathrm{p_T}$ graph for different values of non-extensive parameter using Tsallis Fermi-Dirac Distribution with $O(q-1)^2$.

with these probe particles?". In our model we quantify that all statistics follow the same order and hence we can say that the model is statistically indipendent.

In comparison with the experimental observation we have fitted our model with the experimental data to observe the suppression/enhancement. As it is seen that it describes the experimental data very well. In order to match the theoretical results with the experimental we obtain data in heavy ion collisions at LHC we have taken t_F/τ_R, T, q as an free parameter to fit the data. In Fig. (3.7) it is presented in terms of a nuclear modification factor which exhibits strong suppression in the $\mathrm{p_T}$ range around 6-7 GeV/c. Hence we can say that there is a enegy lose of the heavy quarks due to the medium formation. In present Fig. (3.7) it is presented in terms of a nuclear modification factor which exhibits strong suppression in the $\mathrm{p_T}$ range around 6-7 GeV/c. For increasing q value this suppression becomes higher [62].

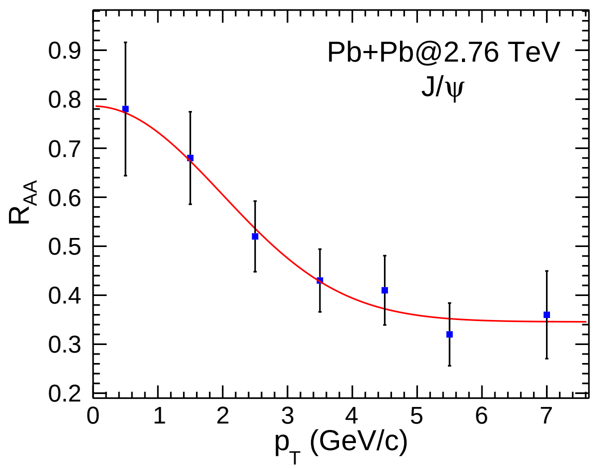

Figure 3.7. Nuclear modification factor R_{AA} versus $\mathrm{p_T}$ with LHC data at 2.76 TeV for $0-90\%$ centrality .

Chapter 4

Summary

As mentioned previously, the Tsallis distribution was derived as the single particle distribution corresponding to a generalization of the Boltzmann-Gibbs entropy through the introduction of the non-extensivity parameter "q". Whereas the Boltzmann-Gibbs distributions are found to apply to systems which exhibit an exponential relaxation in time to a stationary state characterized by exponentials in energy at thermal equilibrium. The generalized form is found to apply to systems which exhibit power laws. In this brief work we have come to the conclusion that our new form of statistics is thermodynamically consistent. In conclusion we have formulated a generalized nonextensive Tsallis entropy and statistics which in the limit $q \to 1$ the familiar BG statistics is recovered. Furthermore, the generalisation has the attractive property of being thermodynamically consistent, and thusly does not violate the four thermodynamic laws deemed characteristic of all systems. This nonextensive Tsallis entropy results in a much better fit to p_T spectra than the associated BG entropy. The Tsallis entropy gives extremely good fits to the single-species particle spectra of various hadrons.

It does however, appear to fall somewhat short when considering combined particle spectra, and this should be further considered. In fact, given that Tsallis distributions appear to fit p_T spectra up to extremely high energies [39], it may be concluded that the hadronization process obeys some generalised statistical process. Within this framework there is still the question of the physical significance of the parameter q. Evidently, one would expect q to depend on the microscopic mechanisms of the system, however a rigorous approach in which a generalised entropy is derived.

In this dissertation, our central goal has been to study and to explore properties of the QGP using heavy quarks (like charm and bottom, as probes) in non-extensive statistics. It has been explained that the heavy quarks, produced quite early(before the formation of QGP medium) in the heavy ion collisions due to the hard scatterings, can be described by the Brownian motion in the thermal bath of light quarks and gluons. The equation describing the motion of heavy quark, i.e. the Boltzmann Transport Equation(BTE) has been discussed and solved in this work. The heavy quark production time is smaller than the QGP lifetime and heavy quarks can pass through the entire evolution of the fireball. The heavy quark equilibration time is of the order of the QGP lifetime, but smaller than the light-quark one. Since the mass of the heavy quark is bigger than the temperature of the medium. Let us summarise the main findings of this discourse and what we have learnt about various properties of QGP.

- The medium of QGP created in the heavy ion collisions, is assumed to be in thermal equilibrium. Heavy quarks, which are produced in the early hard scatterings has been used to probe the properties of QGP. The equation of motion of heavy quark immersed in a QGP fluid can be described by the well-known Boltzmann Transport Equation (BTE). As well solve it in the limits of Non-Extensive statistical mechanics.

- Before calculating the different statistics for heavy quarks, we have solve the BTE in the domain of Relaxation Time Approximation (RTA).

- It is seen that if "q" is increasing consequently R_{AA} is decreasing i.e. by the Eqn. 3.8 it is said that the $f - f_{eq}$ is the collision term which encodes interaction of the probe with the medium. Larger the interaction larger the energy loss, that means larger $f - f_{eq}$ larger the energy loss. That means larger $q \rightarrow$ larger $f - f_{eq} \rightarrow$ larger energy loss $\rightarrow$ smaller R_{AA} value.

- The study of charmonium suppression(J/Ψ) has been done by using our model with experimental data of LHC at 2.76 TeV for $0 - 90\%$ centrality.

We have studied the quarkonium formation in QGP by using the approach based BTE and Relaxation Time Approximation. Measurements of the QGP show it is a short lived state of dense, strongly interacting matter in thermal equilibrium, that rapidly expands and cools. Pb-Pb collisions provide a vital baseline with which we compare our theretical model with experimental data and understand the evolution of the medium.

The above mentioned points are the gist of the work which has been covered in this entire thesis. In view of these findings, we can conclude that, in this dissertation, we were able to illustrate a basic picture of the heavy quark travelling inside the medium of QGP and to develop an idea about various properties of QGP by studying the equation of motion of Heavy quark. In this way the heavy quark successfully can be described as a good probe of the thermalised medium of Quark Gluon Plasma.

The pursuit of knowledge led us to a pathway of illumination where we have tried to learn and discuss the most fundamental questions of all the decades: "How was the universe like at the beginning just after the Big Bang"? and "After the miniature universe has been created due to the heavy ion collisions in the laboratories, how can we describe the medium formed called Quark Gluon Plasma".

Appendix A

Appendix

A.1 Quantum Statistics

In this section we shall briefly describe the formulation of typical statistical mechanics used in the, non-interacting hadron gas, models used to describe the particles generated in heavy-ion collisions. When two heavy-ions collide they produce what is known as a fireball. In the primordial fireball numerous hadrons are created. In such high energy interactions, particle numbers are not conserved. However, it is known that such interactions do conserve the initial quantum number content of the interaction. Furthermore, the centrality of the collision also affects the quantum number content. The quantum numbers usually conserved when performing these calculations are baryon number, B, charge, Q, and strangeness, S and occasionally charm, C. Topness, T , and bottomness b are usually not included as it is reasonable to assume that such heavy quarks are very rarely produced (at these energies). Thus the chemical potential associated with a particular hadron species, i, in the hadron gas at freeze-out is given by $\mu = \mu_b B_i + \mu_Q Q_i + \mu_S S_i + \mu_C C_i$, where $\mu_B, \mu_Q, \mu_S, \mu_C$ are, respectively, the chemical potentials associated with baryon number, charge, strangeness, and charm of the system. Evidently, the net quantum num ber content of the system is given by:

$$B = \sum_i B_i N_i, \;\; 0 = \sum S_i N_i, \;\; Q = \sum_i Q_i N_i, \;\; 0 = \sum_i C_i N_i$$

where N_i is the number of particles of specie i in the hadron gas, and the sum is taken over both particles and anti-particles. There are three statistical ensembles, namely, the micro-canonical (MCE), canonical (CE) and grand canonical (GCE) ensembles that are used extensively. Of these, the MCE is the most restrictive, in that the energy and the quantum numbers in such ensembles are fixed precisely. Somewhat less restrictive is the CE in which relevant quantum numbers remain fixed but the energy; however, is set on average by the temperature, T , of the system. That is to say; if one were to measure the total energy of the system numerous times, these calculated energies would fluctuate around the average energy of the system (determined by the temperature). In the GCE, both the energy and quantum numbers, respectively, are set on average by the temperature, T , and the chemical potentials, where i represents some conserved quantum number. With the appropriate choice of ensemble, one's task is to compute the partition function of the system under consideration. Once evaluated, the partition function can be utilised to calculate the relevant thermodynamic quantities characteristic of the fireball at freeze-out. Generally, in the GCE, the partition function is derived via considering the transfer of energy and particles between a system and a large reservoir. We can obtain the same probability distribution function via the extremization of the Shannon-Gibbs entropy given by:

$$S = -\sum_{i}^{W} p_i \ln p_i \tag{1.1}$$

where the index i labels each unique configuration (microstate) of the system and W represents the total number of possible configurations of the system, with the constraints,

$$f(p_i) = \sum_{i}^{W} p_i = 1, \tag{1.2}$$

$$g(p_i) = \sum_{i}^{W} E_i p_i = \bar{E}, \tag{1.3}$$

$$h(p_i) = \sum_{i}^{W} N_i p_i = \bar{N} \tag{1.4}$$

The given the constraints in (1.2) to (1.4) we seek to maximize the entropy. When maximising a multivariable functional subject to a given number of constraints, the approach used is that of the method of Lagrange multipliers. Consequently, the variational problem that requires solving is:

$$\delta[S(p_i) - \alpha\delta f(p_i) - \beta\delta h(p_i) - \gamma\delta h(p_i)] = 0 \tag{1.5}$$

Evidently (1.5) is merely a compact form of expressing W equations of the form:

$$\ln p_n + 1 = -\alpha - \beta E_n - \gamma N_n \tag{1.6}$$

(1.6) implifies to the following expression for the probabilities of the various states of the system at equilibrium:

$$p_n = Ae^{-(\beta E_n + \gamma N_n)} \tag{1.7}$$

where [1] $A = \exp^{-\alpha-1}$. Moreover, the constraint expressed in (1.2) allows for the reformulation of A into the following :

$$A = \left(\sum_i e^{-(\beta E_i + \gamma N_i)}\right)^{-1} \tag{1.8}$$

Describing the system in terms of its possible macrostates (as opposed to microstates), (1.9) can be reformulated into the more familiar form:

$$\begin{aligned} A &= \left(\sum_{N=0}^{\infty}\sum_i e^{-(\beta E_i + \gamma N_i)}\right)^{-1} \\ &= \frac{1}{Z_{GC}} \end{aligned} \tag{1.9}$$

where the index i now represents the macrostate (defined solely by the energy and not the number of particles of the system) with energy E_i , and N the number of particles (which is run over for each particular macrostate). Hence, we can identify $A = 1/Z_{GC}$ where Z_{GC} is the partition function of

[1] Evidently, this is under the assumption that a configuration is uniquely determined by its energy and number of particles. If not, the degeneracy of the state must be included.

GCE by identifying the parameters $\beta = \frac{1}{T}$ and $\gamma = \beta\mu$. Evidently, we have derived the probability distribution function for the GCE at equilibrium via the extremization of the BG entropy under the constraints expressed in (1.2), (1.3), (1.4), under purely statistical, non-physical, arguments. If the given system is quantum mechanical, then it will be composed of energy levels ϵ_ν each with a given number of particles n , such that $\sum n_\nu \epsilon_\nu = E_n$ and $\sum n_\nu = N$. Using this new prescription, the GC partition function is given by:

$$Z_{GC} = \sum_N^\infty \sum_{\{n_\nu\}}^* \prod_\nu e^{-\beta(\epsilon_\nu n_\nu - \mu n_\nu)} \tag{1.10}$$

$$= \sum_{\{n_\nu\}}^* \prod_\nu e^{-\beta(\epsilon_\nu n_\nu - \mu n_\nu)} \tag{1.11}$$

where $\sum_{\{n_\nu\}} = \sum_{n1} \sum_{n2} .... \sum_{n\alpha}$ and in (1.10) is representative of the constraint: $\sum n\nu = N$. Consequently one can then rewrite (1.11) as:

$$Z_{GC} = \sum_{\{n_\nu\}} \prod_\nu [e^{-\beta(\epsilon_\nu - \mu)}]^{n\nu} \tag{1.12}$$

$$Z_{GC} = \prod_\nu z_\nu \tag{1.13}$$

where z is the partition function for the v^{th} energy level. If the system is composed of fermions then,

$$z_\nu^{FD} = 1 + e^{-\beta(\epsilon_\nu - \mu)} \tag{1.14}$$

If, instead, the system is comprised of bosons, the partition function for energy level ν is given by:

$$z_\nu^{BE} = \sum_{n_{\nu=0}}^\infty (e^{-\beta(\epsilon_\nu - \mu)^{n_\nu}}) \tag{1.15}$$

$$= \frac{1}{1 - e^{-\beta(\epsilon_\nu - \mu)}} \tag{1.16}$$

The average population number of a given quantum state will be given by:

$$\begin{aligned}\langle n_\nu \rangle &= \frac{\sum_{n_\nu=0}^{\infty} n_\nu e^{-\beta(\epsilon_\nu n_\nu - \mu n_\nu)}}{\sum_{n_\nu=0}^{\infty} e^{-\beta(\epsilon_\nu n_\nu - \mu n_\nu)}} && (1.17)\\ &= -\frac{1}{\beta}\frac{\partial \ln z_\mu}{\partial \epsilon_\nu} && (1.18)\end{aligned}$$

which in the case of fermions and bosons is given by:

$$\langle n_\nu \rangle^{FD,BE} = \frac{1}{e^{\beta(\epsilon_\nu - \mu)} \pm 1} \quad (1.19)$$

where the plus and minus signs denote the average occupation number for fermions and bosons respectively. Since the average number of particles is given by:

$$\begin{aligned}N &= -\frac{\partial \Omega}{\partial \mu}\\ &= T\frac{\partial \ln Z^{GC}}{\partial \mu}\\ &= \pm T\frac{\partial \sum_\nu \ln(1 \pm e^{-\beta(\epsilon_\mu - \mu)})}{\partial \mu}\\ &= \sum_\nu \frac{e^{-\beta(\epsilon_\nu - \mu)}}{1 \pm e^{-\beta(\epsilon_\nu - \mu)}}\\ &= \sum_\nu \langle n_\nu \rangle && (1.20)\end{aligned}$$

We can now multiply and divide by a factor of Δp_i , but since $\Delta p_i = 2\pi/L_i$ (quantum mechanical particle in a box with continuous boundary conditions) where $i = x, y, z$ we can rewrite (1.20) as:

$$\bar{N} = \sum_\nu \frac{V}{(2\pi)^3} \langle n_\nu \rangle (\Delta p_x)(\Delta p_y)(\Delta p_z) \quad (1.21)$$

where $V = \prod_i L_i$.Taking the limit where $L_i \to \infty$(the large volume approximation) we find that the average number of particles is given by:

$$\begin{aligned}\bar{N} &= V\int \frac{d^3p}{(2\pi)^3} \langle n_\nu \rangle\\ &= V\int \frac{d^3p}{(2\pi)^3} \frac{1}{e^{\beta(\epsilon - \mu)} \pm 1} && (1.22)\end{aligned}$$

Using the above result, it can be easily shown that the entropy for a gas of identical fermions/bosons is given by:

$$S^{FD,BE} = -\sum_{\nu}[n_\nu \ln n_\nu \pm (1 \mp n_\nu)\ln(1 \mp n_\nu)] \tag{1.23}$$

Evidently, in the Boltzmann limit, i.e. an ideal gas of extremely low concentration or high temperature, the expression for the average occupation number expressed in (1.19) reduces to:

$$\langle n_\nu \rangle^B = e^{-\beta(\epsilon_\nu - \mu)} \tag{1.24}$$

Thus, using the expression for the Boltzmann approximation for the mean occupation number in (1.20), the expression for the entropy in (1.23), in the Boltzmann limit, simplifies to:

$$S^B = -\sum_{\nu}[n_\nu \ln n_\nu - n_\nu] \tag{1.25}$$

One can show naturally in an analogous manner to the previous analysis that the maximization of this particular entropy with respect to the constraints:

$$g = \sum n_\nu \epsilon_\nu = \bar{E} \tag{1.26}$$
$$h = \sum_{\nu} n_\nu = \bar{N} \tag{1.27}$$

The other statistics we can quantify by the following way;

$$S = -\sum p \ln p$$

Using quantum statistics the expression for the entropy is given by:

$$S = -\prod_{\nu}\sum_{n_\nu} \frac{e^{-\beta(\epsilon_\nu - \mu)n_\nu}}{\prod_\alpha z_\alpha} \ln\left(\frac{e^{-\beta(\epsilon_\nu - \mu)n_\nu}}{\prod_\gamma z_\gamma}\right) \tag{1.28}$$

Simplifying the expression in (1.28) we obtain the following:

$$\begin{aligned}
S &= -\prod_{\nu}\sum_{n_\nu}\frac{e^{-\beta(\epsilon_\nu-\mu)n_\nu}}{\prod_\alpha z_\alpha}\left[-\beta(\epsilon_\nu-\mu)n_\nu-\ln\left(\prod_\gamma z_\gamma\right)\right] \\
&= \prod_{\nu}\sum_{n_\nu}\frac{\beta(\epsilon_\nu-\mu)n_\nu e^{-\beta(\epsilon_\nu-\mu)n_\nu}}{\prod_\alpha z_\alpha}+\prod_{\nu}\sum_{n_\nu}\frac{\ln\left(\prod_\gamma z_\gamma\right)e^{-\beta(\epsilon_\nu-\mu)n_\nu}}{\prod_\alpha z_\alpha} \\
&= \prod_{\nu}\sum_{n_\nu}\frac{\beta(\epsilon_\nu-\mu)n_\nu e^{-\beta(\epsilon_\nu-\mu)n_\nu}}{\prod_\alpha z_\alpha}+\ln\left(\prod_\gamma z_\gamma\right) \qquad (1.29)
\end{aligned}$$

But the first term in (1.29) can be expressed as a partial derivative, namely:

$$T\frac{\partial\ln(\prod_\nu z_{\{nu\}})}{\partial T}=\prod_{\nu}\sum_{n_\nu}\frac{\beta(\epsilon_\nu-\mu)n_\nu e^{-\beta(\epsilon_\nu-\mu)n_\nu}}{\prod_\alpha z_\alpha} \qquad (1.30)$$

As such using (1.29) we can rewrite (1.29) as the following:

$$\begin{aligned}
S &= T\frac{\partial\ln(\prod_\nu z_\nu)}{\partial T}+\ln\left(\prod_\gamma z_\gamma\right) \\
&= \frac{\partial}{\partial T}T\ln\left(\prod_\nu z_\nu\right) \\
&= \frac{\partial}{\partial T}(T\ln Z_{GC}) \qquad (1.31)
\end{aligned}$$

We know that for fermions and bosons $Z_{GC}^{FD,BE}=\prod_\nu(1\pm e^{-\beta(\epsilon_\nu-\mu)})^{\pm 1}$, therefore:

$$\ln Z_{GC}^{FD,BE}=\pm\sum_\nu\ln(1\pm e^{-\beta(\epsilon_\nu-\mu)}) \qquad (1.32)$$

Thus the entropy is given by:

$$
\begin{aligned}
S_{GC}^{FD,BE} &= \sum_{\nu}\left\{\ln(1\pm e^{-\beta(\epsilon_\nu-\mu)})^{\pm 1}+\beta(\epsilon_\nu-\mu)\left(\frac{e^{-\beta(\epsilon_\nu-\mu)}}{1\pm e^{-\beta(\epsilon_\nu-\mu)}}\right)\right\} \qquad (1.33)\\
&= \sum_{\nu}\left\{\mp\left(\frac{1}{1\pm e^{-\beta(\epsilon_\nu-\mu)}}\right)+\left(\frac{\beta(\epsilon_\nu-\mu)}{e^{\beta(\epsilon_\nu-\mu)}\pm 1}\right)\right\}\\
&= \sum_{\nu}\left\{\mp\left[\ln\left(\frac{e^{\beta(\epsilon_\nu-\mu)}}{e^{\beta(\epsilon_\nu-\mu)}\pm 1}\right)\right]+\left(\frac{\beta(\epsilon_\nu-\mu)}{e^{\beta(\epsilon_\nu-\mu)}\pm 1}\right)\right\}\\
&= \sum_{\nu}\left\{\mp\left[\left(\frac{e^{\beta(\epsilon_\nu-\mu)}\pm 1}{e^{\beta(\epsilon_\nu-\mu)}\pm 1}\right)\ln\left(\frac{e^{\beta(\epsilon_\nu-\mu)}}{e^{\beta(\epsilon_\nu-\mu)}\pm 1}\right)\right]\left(\frac{\beta(\epsilon_\nu-\mu)}{e^{\beta(\epsilon_\nu-\mu)}\pm 1}\right)\right\}\\
&= \sum_{\nu}\left\{-\frac{1}{e^{\beta(\epsilon_\nu-\mu)}\pm 1}\ln\left(\frac{1}{1\pm e^{\beta(\epsilon_\nu-\mu)}}\right)\right\}\\
&- \sum_{\nu}\left\{\frac{\beta(\epsilon_\nu-\mu)}{e^{\beta(\epsilon_\nu-\mu)}\pm 1}\mp\frac{e^{\beta(\epsilon_\nu-\mu)}}{e^{\beta(\epsilon_\nu-\mu)}\pm 1}\ln\left(\frac{e^{\beta(\epsilon_\nu-\mu)}}{e^{\beta(\epsilon_\nu-\mu)}\pm 1}\right)+\left(\frac{\beta(\epsilon_\nu-\mu)}{e^{\beta(\epsilon_\nu-\mu)}\pm 1}\right)\right\}
\end{aligned}
$$

Hence we get

$$S_{GC}^{FD,BE}=-\sum_{\nu}\left\{n_\nu\ln n_\nu\pm(1\mp n_\nu)\ln(1\mp n_\nu)\right\} \qquad (1.34)$$

A.2 Kinematics

We introduce the basic kinetic variables used in high energy heavy-ion collisions.

The energy in the CM frame can be calculated using the 4-vectors $\mathbf{E}$(E,0,0,p_z). It is simply;

$$E_{CM}=\sqrt{(E^\mu+E^\nu)^2}=\sqrt{(2E)^2} \qquad (1.35)$$

i.e. twice the beam energy. Usually the CM energy is denoted as $\sqrt{s_{NN}}$. For heavy ion collision $\sqrt{s_{NN}}$ is often used instead, the $\sqrt{s_{NN}}$ implies the energy per nucleon pair. Using the available energy per nucleon pair makes it easier to compare heavy ion experiments with different kinds of nuclei.

Transverse Momentum & Energy

Often the momentum is divided into two terms. A transverse momentum, and a p_z momentum.The transverse momentum has the advantage of being Lorentz invariant. It is defined as:

$$p_T = \sqrt{p_x^2 + p_y^2} \tag{1.36}$$

The transverse mass is defined as:

$$m_T = \sqrt{m_0^2 + p_T^2} \tag{1.37}$$

where m_0 is the rest mass of the particle. Energy of a given particle is defined through the relativistic formula:

$$E \ = \sqrt{m_T^2 + p_z^2}. \tag{1.38}$$

Rapidity

In relativity, rapidity denoted by y is commonly used as a measure for relativistic velocity. For one-dimensional motion, rapidities are additive whereas velocities must be combined by Einstein's Velocity-addition formula. For low speeds, rapidity and velocity are proportional, but for higher velocities, rapidity takes a larger value, the rapidity of light being infinite.

$$y \ = \ \frac{1}{2} \ln \frac{E + p_z}{E - p_z}, \tag{1.39}$$

where p_z is the component of momentum along the beam axis. Rapidity has the advantage of being additively invariant under Lorentz transformations, while p_z is not. This is the rapidity of the boost along the beam axis which takes an observer from the lab frame to a frame in which the particle moves only perpendicular to the beam. This also means that y is Lorentz invariant.

$$\begin{aligned} E &= m_T \cosh y \\ p_z &= m_T \sinh y \end{aligned} \quad (1.40)$$

Pseudorapidity

In experimental particle physics, pseudorapidity, η, is a commonly used spatial coordinate describing the angle of a particle relative to the beam axis. It is defined as:

$$\eta \equiv -\ln\left[\tan\theta/2\right]$$

where where $\tan(\theta) = \sqrt{x^2 + y^2/z}$ is the angle between the particle three-momentum $\mathbf{p}$ and the positive direction of the beam axis. Inversely,

$$\theta = 2arc\tan(e^{\eta})$$

As a function of three-momentum $\mathbf{p}$, pseudorapidity can be written as;

$$\eta = \frac{1}{2}\ln\left(\frac{|p| + p_L}{|p| - p_L}\right) = arc\tanh\frac{p_L}{|p|}$$

where $|p| = p_T\cosh\eta$, $p_z = p_T\sinh\eta$ & p_L is the component of the momentum along the beam axis (i.e. the longitudinal momentum - using the conventional system of coordinates for hadron collider physics, this is also commonly denoted p_z).

Invariant Yeild

The differential invariant yield section is defined as the number of particles in a phase space segment, which is commonly described in cylindrical coordinates.

$$
\begin{aligned}
E\frac{d^3N}{dp^3} &= \frac{d^3N}{p_x dp_y dp_z} \\
&= \frac{d^3N}{p_T dp_T d\phi dz} \\
&= \frac{d^2N}{2\pi p_T dp_T dz} \\
&= \frac{d^2N}{2\pi p_T dp_T m_T d(m_T \sinh y)} \\
&= \frac{d^2N}{2\pi p_T dp_T m_T \cosh y dy} \\
&= \frac{d^2N}{2\pi p_T dp_T dy} \qquad (1.41)
\end{aligned}
$$

$$
\begin{aligned}
\frac{dp_T}{dm_T} &= \frac{d\sqrt{m_T^2 - m_0^2}}{dm_T} \\
&= \frac{2m_T}{2p_T} \\
dp_T &= \frac{m_T}{p_T} dm_T \\
\frac{d^3N}{dp^3} &= \frac{d^2N}{2\pi E m_T dm_T dp_T dy} \qquad (1.42)
\end{aligned}
$$

Bibliography

[1] L. Evans, P. Bryant, "LHC Machine", **JINST 3 (2008)**, p. S08001

[2] A. A. Alves et al., "The LHCb Detector at the LHC", **J. Instrum. 3 (2008)**, p. S08005

[3] R. Stock, "Relativistic Heavy Ion Physics: Introduction", vol. **23**, Springer Materials

[4] CERN-press-office, "New State of Matter created at CERN"

[5] T. H. Kohsuke Yagi, Y. Miake, "Quark-Gluon Plasma", Cambridge University Press, 2005

[6] "NASA", url: http://map.gsfc.nasa.gov/media/060915

[7] H. von Gersdorff, L. McLerran, M. Kataja, and P. V. Ruuskanen, Phys. Rev. D34 (1986) 794; M. Kataja, P. V. Ruuskanen, L. McLerran, and H. von Gersdorff, Phys. Rev. D34 (1986) 3755

[8] J. Alam, P. Roy, S. Sarkar, S. Raha and B. Sinha, Int. J. Mod. Phys. A12 (1997)

[9] P. Roy, J. Alam, S. Sarkar, B. Sinha and S. Raha, Nucl. Phys. A 624 (1997) 687

[10] C.MichaelL.Vanryckeghem J. Phys. G 3 1977 L **151**

[11] C. Alcock, The Astrophysics and Cosmology of Quark-Gluon Plasma, in Quark-Gluon Plasma, Springer-Verlag (1990)

[12] On QGP Formation in pp Collisions at 7 TeV Fu-Ming Liu, Klaus Werner

[13] Radial flow in non-extensive thermodynamics and study of particle spectra at LHC in the limit of small (q - 1) Trambak Bhattacharyy Eur. Phys. J. A (2016) 52

[14] J. Bjorken, FERMILAB-PUB-82-059-THY **(1982)**

[15] The STAR Collaboration, J. Adams et al., Nucl. Phys. **A757** (2005) 102, nucl-ex/0501009

[16] The PHENIX Collaboration, K. Adcox et al., Nucl. Phys. **A757** (2005) 184, nucl-ex/0410003

[17] The ALICE Collaboration, K. Aamodt et al., Phys. Lett. **B696** (2011) 30, nucl-ex/1012.1004

[18] T. Matsui and H. Satz, Phys. Lett. **B178** (1986) 416

[19] The NA50 Collaboration, B. Alessandro et al., Eur. Phys. J. **C39** (2005) 335, hep-ex/0412036

[20] The PHENIX Collaboration, A. Adare et al., Phys. Rev. Lett. 98 (2007) **232301**, nucl-ex/0611020

[21] The ALICE Collaboration, B. Abelev et al., Phys. Rev. Lett. 109 (2012) **072301**, hep-ex/1202.1383

[22] R.L. Thews, M. Schroedter and J. Rafelski, Phys. Rev. C63 (2001) 054905, hep-ph/0007323

[23] P. Braun-Munzinger and J. Stachel, th/0007059

[24] H. Satz, The Search for the QGP: A Critical Appraisal, Nucl. Phys. Proc. Suppl.**94** (2001) 204-218

[25] M. Gyulassy, I. Vitev, X.-N. Wang, and B.-W. Zhang, Jet Quenching and Radiative Energy Loss in Dense Nuclear Matter, arXiv:nucl-th/0302077v2 2003

[26] A. Kovner and U. A. Wiedemann, Gluon Radiation and Parton Energy Loss, arXiv:hep-ph/0304151v1 (2003)

[27] X.-N. Wang and M. Gyulassy, Gluon shadowing and jet quenching in A+A collisions at $\sqrt{s_{NN}} = 200$A GeV, Phys. Rev. Lett. 68, 1480-1483 (1992)

[28] S.S. Adler *et al*, Phys. Rev. Lett. **91**, 072303 (2003)

[29] T. Affolder *et al.*, Phys. Rev. D **65**, 092002 (2002)

[30] T. Bir o, Z. Schram, and K. Urm,Physics **37**, 094027 (2010)

[31] E. Fermi, Thermodynamics (Dover Publications, Inc. New York, 1956)

[32] F. Reif, Fundamentals of Statistical and Thermal Physics (McGraw-Hill, 1965)

[33] L. Reichl, A Modern Course in Statistical Physics (Wiley-VCH, 2004).

[34] S. R. de Groot, W. A. van Leeuwen, C. G. van Weert

[35] E-802 Collabohration *et al.*, Phys. Rev. C**52**,1995

[36] A. Andronic, P. Braun-Munzinger, and J. Stachel, Nuclear Physics A 772, 167

[37] A. Plastino, C. Tsallis, Physica A **261**,534 (1998)

[38] C.Tsallis J. Stat **52**, 479(1988)

[39] Braz. J. Phys. vol.**37** no.2c Sao Paulo June 2007

[40] C. Beck, Phys.Rev.Lett.,**87** 2001

[41] CMS Collaboration,CMSPASHIN-12-014(2014)

[42] C.Beck Phys.RevLett.**87**.180601

[43] J. Adams, C. Adler, M. Aggarwal, et al. Identified Particle Distributions in pp and Au+Au Collisions at $\sqrt{s}_{NN} = 200$ GeV, Phys.Rev.Lett,**92**(11)

[44] Highly relativistic nucleus-nucleus collisions: The central rapidity region. Phys.Rev D,**27**

[45] T.S Biro and Berndt Muller. Almost exponential transverse spectra from power law spectra.(2004)

[46] G. Wilk and Z. Woldarczyk. Interpretation of the Nonextensivity Parameter q in Some Applications of Tsallis Statistics and Levy Distributions. Phys.Rev.Lett **84**(13), 2000

[47] Z. W lodarczyk and G. Wilk, Eur. Phys. J. A **40**, 299 (2009)

[48] Z. W lodarczyk and G. Wilk, Eur.Phys.J. A**48**, 161 (2012), 1203.4452

[49] I. Sena and A. Deppman, Eur.Phys.J. A49, 17 (2013), 1209.2367

[50] K. Urmossy, arXiv preprint arXiv:1212.0260 (2012)

[51] T. Biro and G. Purcsel, Phys.Rev.Lett. 95, **162302** (2005), hep-ph/0503204

[52] A. Adare, S. Afanasiev, C. Aidala, et al. Identified charged hadron production in pp collisions at 200 and 62.4 GeV.Physical Review C,**83**(6)2011

[53] V. Khachatryan, a. M. Sirunyan, A. Tumasyan, et al. Strange particle production in pp collisions at 0.9 and 7 TeV.JHEP, 2011

[54] S Uddin, Hindawi, 154853, 2015

[55] R. Hagedorn, Riv. Nouvo Cimento **6**, 1 (1984)

[56] Phys.Rev.D **92**, 074009 (2015)

[57] M.J Tannenbaum,J.Kang,E802 Collaboration

[58] J.Cleymans, A.S Parvan, Phys.Lett.B, vol**723**

[59] J. Cleymans and D. Worku EPJC **1203** 2012

[60] Gyulassy M 2002 Lect.NotesPhys. **583** 37

[61] Quark-gluon Plasma 4, Rudolph C. Hwa, Xin-Nian Wang, $WorldScientific$

[62] S. Tripathy, T. Bhattacharyya, P. Garg, Prateek Kumar, R. Sahoo, J. Cleymans, arxiv:1606.06898

[63] McGraw Hill Encyclopaedia of Physics (2nd Edition), C.B. Parker, 1994